PERFORMANCE ANALYSIS OF PHOTOGRAMMETRY TECHNIQUE IN 3D MODEL REVERSE ENGINEERING

By
BINAY HALDAR
B.Tech in Mechanical Engineering
Kanksa Academy of Technology& Management
West Bengal University of Technology

Examination Roll No.: M4PRD22008
Registration No.: 154476 of 2020-2021

THESIS
SUBMITTED IN PARTIAL FULFILLMENT OF THE REQUIREMENT FOR THE AWARD OF THE DEGREE OF MASTER OF PRODUCTION ENGINEERING IN THE FACULTY OF ENGINEERING AND TECHNOLOGY,
JADAVPUR UNIVERSITY

DEPARTMENT OF PRODUCTION ENGINEERING
JADAVPUR UNIVERSITY
KOLKATA-700032

JADAVPUR UNIVERSITY FACULTY OF ENGINEERING AND TECHNOLOGY

CERTIFICATE OF RECOMMENDATION

WE HEREBY RECOMMEND THAT THE THESIS ENTITLED **"PERFORMANCE ANALYSIS OF PHOTOGRAMMETRY TECHNIQUE IN 3D MODEL REVERSE ENGINEERING** " BE CARRIED OUT UNDER MY/OUR GUIDANCE BY **MR. BINAY HALDAR** MAY BE ACCEPTED IN THE PARTIAL FULFILLMENT OF THE REQUIREMENTS FOR THE DEGREE OF "MASTER OF PRODUCTION ENGINEERING".

_____

(Prof. Soumya Sarkar)
Thesis Advisor
Dept. of Production Engineering
Jadavpur University
Kolkata-700032

_____

HEAD, Dept. of Production Engineering
Jadavpur University
Kolkata-700032

_____

DEAN, Faculty of Engineering and Technology
Jadavpur University
Kolkata-700032

JADAVPUR UNIVERSITY
FACULTY OF ENGINEERING AND TECHNOLOGY

CERTIFICATE OF APPROVAL

The foregoing thesis is hereby approved as a creditable study of an engineering subject carried out and presented in a manner satisfactory to warrant its acceptance as a pre-requisite to the degree for which it has been submitted. It is understood that by this approval, the undersigned doesn't necessarily endorse or approve any statement made, opinion expressed and conclusion drawn therein but thesis only for the purpose for which it has been submitted.

_____

COMMITTEE ON
FINAL EXAMINATION
FOR EVALUATION OF
THE THESIS

(External Examiner)

_____

(Internal Examiner)

ACKNOWLEDGEMENT

While bringing out this thesis to its final form, I came across several people whose contributions in various ways helped my field of project work and they deserve special thanks. It is a delight to convey my gratefulness to all of them. First and foremost, I would like to express my deep sense of gratitude and indebtedness to my supervisor Prof. Soumya Sarkar, Professor of the Production Engineering Department at Jadavpur University for his priceless and meticulous supervision at every phase of my work inspired me in innumerable ways.

I would like to express my warmest gratitude to all respected teachers in this department for helping me with variable suggestions.

I also want to express my heartiest thanks to Kingshuk Mandal and Subham Biswas, research scholars of the Production Engineering Department and Prof. Souren Kumar Saren, Assistant Professor, Production Engineering Department, Jadavpur University for their cordial assistance throughout my thesis work.

Any omission in this brief acknowledgement does not mean a lack of gratitude.

_____

BINAY HALDAR
Class Roll No: 002011702009

Table of Content

Chapter 1

1. Introduction

The basic principle of 3D scanning is to use a 3D scanner to collect data about a subject. Some 3D scanners can simultaneously collect shape and colour data. A 3D scanned colour surface is called a texture. 3D scans are compatible with Computer-Aided Design (CAD) software and also 3D printing, after preparing the 3D model via specific software. A 3D scan can give a lot of information about the design of an object, in a process called reverse engineering [1].

3D scanning is a technology for creating high-precision 3D models of real-world objects. This 3D model consists of a polygon mesh or point cloud of geometric samples on the surface of the subject. These points can then be used to extrapolate the shape of the subject (a process called reconstruction). If colour information is collected at each point, then the colours or textures on the surface of the subject can also be determined. A 3D scanner takes multiple snapshots of an object. The shots are then fused into a 3D model, an exact three-dimensional copy of the object. 3D scanning is a technology used in cutting-edge workflows. 3D scanners are used in a range of industries, from manufacturing to healthcare and VR. Retrofitting heavy machinery, performing quality control of mechanical parts, designing customized prosthetic devices, creating visual effects for movies, and developing characters for video games – all such projects have high-precision 3D models of physical objects at their core. Many different 3D scanning technologies exist to 3D scan objects, environments, and people. Each 3D scanning technology comes with its limitations, advantages, and costs [2].

3D scanning technology is largely classified into the following methods:
Time of Flight, Triangulation, Phase shift, Stereo.
Different types of 3d scanning methods and the principles they are based on are as follows:

1. LASER triangulation 3D scanning technology.
2. Structured light 3D scanning technology.
3. Photogrammetry.
4. Contact-based 3D scanning technology.

1.1 Laser pulse-based 3D scanning technology

Laser-based 3D scanners use a process called trigonometric triangulation to accurately capture a 3D shape as millions of points. Laser scanners work by projecting a laser line or multiple lines onto an object and then capturing its reflection with a single sensor or multiple sensors. The sensors are located at a known distance from the laser's source. Accurate point measurements can then be made by calculating the reflection angle of the laser light. Laser scanners are very popular and come in many designs.

They include handheld portable units, arm-based, CMM-based, long-range, and single-point long-range trackers.

Benefits of 3D Laser Scanners

1. Scan tough surfaces, such as shiny or dark finishes
2. Lesser sensitive: to changing light conditions and ambient light
3. Portable
4. Simple design, easy to use, and low cost.

1.2 Projected or Structured Light 3D Scanners

Historically known as “white light” 3D scanners, mainly structured light 3D scanners today use a blue or white LED projected light. These 3D scanners project a light pattern consisting of bars, blocks, or other shapes onto an object. The 3D scanner has one or more sensors that look at the edge of those patterns or structural shapes to determine the object's 3D shape.

The distance from the sensors to the light source is known using the same trigonometric triangulation method as laser scanners. Structured light scanners can be tripod mounted or handheld.

Benefits of Structured light 3D Scanners

1. Very fast scan times –as fast as 2 seconds per scan
2. Large scanning area –as large as 48 inches in a single scan
3. High resolution –as high as 16 million points per scan and 16-micron (.00062”) point spacing
4. Very high accuracy –as high as 10 microns (.00039”)
5. Versatile –multiple lenses to scan small to large parts in a single system
6. Portable –handheld systems are very portable
7. Eye safe for 3D scanning of humans and animals
8. Various price points from low cost to expensive depending on resolution and accuracy

1.3 Medium and Long-Range 3D Scanners

Long-range 3D scanners come in two major formats: pulse-based and phase shift–both well suited for large objects such as buildings, structures, aircraft, and military vehicles. Phase shift 3D scanners also work well for medium-range scan needs such as automobiles, large pumps, and industrial equipment. These scanners capture millions of points by rotating 360 degrees while spinning a mirror that redirects the laser outward towards the object or areas to be 3D scanned.

Laser pulse-based 3Dscanners

Laser pulse-based scanners, also known as time-of-flight scanners, are based on a very simple concept: the speed of light is known very precisely. Thus, if the length of time the laser takes to reach an object and reflect a sensor is known, the distance from the sensor to the object is known. These systems use circuitry that is accurate to picoseconds to measure the time it takes for millions of pulses of the laser to return to the sensor and calculates a distance. By rotating the laser and sensor (usually via a mirror), the scanner can scan up to a full 360 degrees around itself.

Laser Phase-shift 3D Scanners

Laser phase-shift systems are another type of time-of-flight 3D scanner technology and conceptually work similarly to pulse-based systems. In addition to pulsing the laser, these systems also modulate the power of the laser beam, and the scanner compares the phase of the laser sent out and returned to the sensor. Phase shift measurements are typically more accurate and quieter but are less flexible for long-range scanning than pulse-based 3D scanners. Laser pulse-based 3D scanners can scan objects up to 1000m away while phase shift scanners are better suited for scanning objects up to 300m or less.

Benefits Long Range 3D Scanners

1. 3D Scan millions of points in a single scan –up to 1 million points per second
2. Large scanning area of more than 1000 Sq. meters
3. Good accuracy and resolution based on object size
4. Non-contact to safely scan all types of objects
5. Portable

1.4. Photogrammetry

This technology is quite simple. It involves stitching together photographs of an object taken from different angles. The photos are taken using a camera or even your smartphone with specific camera settings, while the stitching of those photos is done by special software. The software identifies pixels that correspond to the same physical point and brings pictures together accordingly.

Parameters like the focal length of the lens and its distortion need to be fed into the software by the user to create an accurate model. Photogrammetry is so simple that you can pick up your phone right now and start taking pictures.

The big advantage of using photogrammetry is its accuracy level and the speed with which an object's data is acquired. The downside of this technique is the time it takes to run the image data through the software and the sensitivity of the result to the resolution of the photographs. You need to have a good camera with high resolution and DPI to get a good result.

We can simulate these photos with many software such as Reality capture, Blender, Mushroom, 3DF Zephyr, Agisoft Metashape, etc.

1.5 Contact Scanning

This scanning method involves the physical contact of a probe onto the surface of the object being scanned. First, the object is firmly held in place so that it does not move.

Then, the touching probe is moved all over the object to collect the details of the object and all the 3D information that is necessary to create a digital file.

Enough points on the surface need to be sampled to create an accurate model. Sometimes, an articulated arm is used to control the touching probe and capture multiple angles/configurations with high precision.

Since contact scanning involves actual physical contact with the surface of the object being scanned, even transparent and reflective surfaces can be accurately scanned using this method. This is the major benefit of this technique over other scanning technologies, which as pointed out above, are incapable of scanning such surfaces.

The disadvantage of contact 3D scanning is its slow speed. Running the touching probe through all sections of an object to collect all the 3D information takes time.

Contact 3D scanning is interestingly used to perform quality control in industrial fabrication. Parts that have been newly fabricated can be checked for any deformations or damages using contact scanning [3].

Coordinate Measuring Machine (CMM)

A coordinate measuring machine (CMM) is used primarily to inspect parts. The machine can be controlled manually or through controlled offline through software and computers. Measurements are defined by attaching a probe to the machine. The probe typically has a small ball at the end of a shaft of a known diameter. The CMM is then programmed to contact the part. When the machine senses contact with the probe tip a measurement value is taken in XYZ space. The most common type of CMM is a bridge type which has 3 axis X, Y & Z. The probing system that is attached many times can rotate providing an additional 3 axis for a total of 6 degrees of freedom (DOF). To accurately measure parts to a few microns, CMMs are typically deployed in a controlled inspection room that includes a reinforced floor, controlled humidity and temperature, and isolation from vibration and other forces that could affect the accuracy. In addition, most CMMs have a large granite table surface that is perfectly level. Parts are fixtured onto the granite table so that there is no movement during the measuring process.

Benefits of CMM's

I. One of the most accurate ways of measuring an object. Small to large parts can be measured with the proper machine
II. Industry standards and certifications for measurements and software exist
III. Many styles and sizes of machines exist from many manufacturers [2].

1.6 Various laser Scanners on the market

1.6.1 3D Scanner 2.0 from XYZprinting

Taiwanese manufacturer, XYZprinting, offers one of the more low-cost 3D scanners, the portable and high-resolution 3D Scanner 2.0. The scanner can scan objects that are 5 x 5 x 5 ~ 100 x 100 x 200 cm using an Intel® RealSense™ Camera. The scan resolution is also superior to the 1.0A, between 0.2 and 1.5 mm with an operating range ranging from 25 to 60 cm. The manufacturer also provides XYZScan Handy, a scanning and post-editing software to edit your models after scanning. The product is lightweight measuring 41 x 157 x 61 mm with a weight of 238 g. It is available for €199.

1.6.2 Structure Sensor from Occipital

The Structure Sensor solution adds precise 3D vision to your mobile device, enabling 3D scanning among other features. The only equipment you will need for this 3D scanner to work is an iPad, then once you have downloaded the app Skanect Pro, it will work instantly.

The new version of this device is smaller than the last, 109mm x 18mm x 24mm, and weighs about 65 g. Using it in a 0.3 m to 5m scanning range is recommended. Some other features of this device include indoor mapping and virtual reality gaming! The Structure Sensor retails for $527.

1.6.3 POP 3D Scanner from Revopoint

The Revopoint POP is unique among 3D scanners as it is part of the highest crowdfunded campaign for a 3D scanner on Kickstarter, raising more than USD 2.28 million. It was developed by Revopoint, a company founded in 2014 by a group of young doctors and researchers from MIT, Kent University, and other higher education institutions when they decided to focus on developing easy-to-use and cost-effective 3D scanners. It is safe to say that they certainly succeeded with their POP 3D scanner.

A binocular structured light 3D scanner that uses infrared as its light source, the Revopoint POP is a full-colour scanner with an accuracy of up to 0.3mm, texture scan, and an 8Fps scanning speed. It has several interesting features, including the fact that it is easy to use outdoors because it's portable and can be powered by a power bank. With a cost of the scanner of only $549 in the USA and about $599 in Europe, it is one of the most affordable options on our list, all while still being an effective, precise, high-resolution scanner. Not to mention, it can be used by a variety of users, as it supports four OS platforms – Windows, Android, Mac, and iOS.

1.6.4 Creality CR-Scan 01

Known for its affordable desktop 3D printers, manufacturer Creality has also developed a low-cost 3D scanner, the CR-Scan 01. Weighing only 1.91 kilos, this portable scanner is easy to handle and offers a scanning area of 536 x 378 mm. You will be able to scan your objects with an accuracy of up to 0.1 mm and export them in stl or obj format. Several scanning modes are offered, either manual or on a turntable. It is currently available for 589 €.

1.6.5 SOL 3D Scanner from Scan Dimension

This scanner was developed by Scan Dimension, based in Denmark, and is essentially a hybrid solution. It uses a combination of laser triangulation and white light technology to 3D scan real-life objects. The SOL 3D scanner can provide a resolution of up to 0.1 mm. The 3D scanning process is automated and you can choose between a near and far scanning mode.

The SOL 3D scanner also includes software to simplify your entire workflow. In a few steps, you will be sending your 3D model to your 3D printer. This is a solution meant for makers, hobbyists, educators, and entrepreneurs who may not have the most experience with 3D scanning devices but still want to achieve great results. The SOL 3D scanner retails for $699.

1.6.6 V2 from Matter & Form

The Matter and Form 3D Scanner V2 is a desktop 3D scanning solution manufactured by Matter & Form, a company founded in 2013. This company has made it its mission to develop and distribute affordable, high-resolution 3D scanners. With the V2, it has achieved that mission: the 3D scanner is available for $750 and is capable of producing high-quality scans with an accuracy of up to 0.1 mm. It weighs 1.71 kilograms (3.77 lbs) and has a height of 35.5 cm (13.5 in) and a width of 21 cm (8.25 in). The slim and foldable design allows the device to fit on small desks. The V2 allows the scanning of objects with a maximum height of 25 cm (9.8 in) and a diameter of 18 cm (7.0 in). Windows and Mac scan files are supported, with multiple export options for 3D printing as well.

1.6.7 RangeVision NEO

The NEO 3D scanner from the manufacturer RangeVision is an entry-level device with two 2-megapixel cameras, which works using Structured Light Scanning (SLS) technology. With an automatic scan mode, the scanner is suitable for all those who have little experience in digitizing objects. The SLS-3D scanner can capture objects from 30mm to 1200mm with a precision of 0.05mm, with 3D scans created using RangeVision software. Also included is a turntable and tripod, which make scanning easier for the user. According to the manufacturer, the NEO's scans are suitable for reverse engineering, 3D modelling, historic preservation, and, of course, 3D printing. The RangeVision NEO is available for around €2,190, making it one of the few low-cost desktop 3D scanners available.

1.6.8 iReal 2E from ScanTech

iReal 2E is a professional handheld colour 3D scanner manufactured by ScanTech. The company specializes in developing, manufacturing, and selling intelligent visual inspection equipment and counts an entire range of 3D scanners for various applications and sectors. The iReal 2E is designed for medium to large-sized objects and human body 3D scanning.

In terms of technology, the iReal 2E colour 3D scanner adopts the infrared VCSEL structured light technology. Without attaching markers, quick texture capturing and geometry acquisition can be achieved, and mixed alignment modes meet various scanning situations. Additionally, this 3D scanner offers algorithm functions, easy-to-use software, ergonomic design, and durability for accurate 3D measurement in colour.

1.6.9 Caliber, the low-cost 3D scanner, from Thor3D

Thor3D is a Russian manufacturer that is behind the Caliber portable 3D scanner. Based on structured light technology, it integrates a touch screen so that the user can follow the points it captures in real time. It offers accuracy down to 0.1 mm and is capable of scanning objects from 30 cm to 10 meters long. Black and glossy surfaces can be easily scanned and exported in STL, obj, ply, or WRML formats. Finally, the Caliber is fast and convenient, capable of scanning up to 3 million points per second and weighing only 900 grams. It is available for 4,990 euros.

1.6.10 EINSCAN H from Shining 3D

The EinScan H is one of the most advanced versions of portable 3D scanners developed by the Chinese manufacturer Shining3D. Based on the hybrid structure light technology of LED and invisible infrared light, the EinScan H can perform human face scans more comfortably and without emitting strong light. It also incorporates a full-colour camera and a large field of view for a truly impressive final quality of the models, ready for processing in just a few minutes. Its high resolution of 0.25 mm and data accuracy down to 0.05 mm make this a good choice in the market considering the price/performance ratio. In addition, it stands out for its light weight of almost 700g and intuitive user interface. The base price of this model is $5000.

1.6.11 Eva Lite from Artec 3D

Artec 3D, based in Luxembourg, offers the Eva Lite as its cheapest option for 3D scanning. This professional scanner is specialized in the digitization of complex geometries, such as the human body, and is therefore increasingly used in the medical field. It works based on structured light technology and, although it cannot capture colours and textures like most scanners of the brand, it has an accuracy of 0.5 mm.

This 3D scanner works with the software package Artec Studio. Artec Studio is a powerful tool for an optimized 3D scanning process. This software can perform, assemble and repair 3D scans. It is currently available for $9,800.

1.6.12 Phiz 3D scanner

The Phiz 3D scanner by Kiri Innovations is an exciting budget approach to 3D scanning, as it builds on the powerful cameras and computing power already in today's mobile phones. As phone cameras have become more and more powerful, integrating depth sensors and other extras, a 3D scanner that utilizes your phone's scanning potential is the ideal lightweight accessory to create accurate 3D models you can use or 3D print. The Phiz 3D scanner comes with a turntable that connects to your phone and wirelessly instructs it to rotate the object so you can scan it in 3D. The other part is a 5mW laser that helps scan the object during laser triangulation and can adjust lighting conditions to make sure your model is captured clearly. With the 3DScanLink app, your scans are processed and can be exported in STL and OBJ formats.

Kiri says that its patented technology allows for a fully adjustable scan range as fixed distances between the camera, laser, and turntable are no longer needed. You can scan any object between 50 mm^3 and 400 mm^3 – as long as it's under 2kg. Basic scans take 4-10 minutes, while super high-quality scans will take up to half an hour. The accuracy of the scanner is 0.2mm and the market price is $379

1.6.13 Shinning 3D Einscan SP

Several scanners from Chinese manufacturer Shining 3D make our list, but among their most affordable is the EinScan SP desktop scanner. It's capable of scanning with or without a turntable, enabling you to capture objects of a wide range of sizes. Using white light makes this scanner safe and easy to use. Shining also makes 3D printers and offers an attractive education bundle that includes a 3D scanner, 3D printer, educational course materials, and supplies.

The EinScan SP has a high scan accuracy of up to 0.05mm and can detect a vast range of colours and textures. Although the EinScan SP is certainly impressive in its own right, the software is what makes this scanner shine. The EinScan software is exceptionally stable and has an easy-to-use interface, but you will need a good processor to calculate the meshes quickly. The software has functions that enable you to fill holes in your mesh, smooth and sharpen objects, and can also readjust the data coordinates in the post-processing process to provide more perfect 3D data for subsequent applications. The market price of the scanner is $1699 [3].

1.6.14 L100

The Nikon Metrology L100 is the next-generation CMM laser scanner, offering the best possible combination of speed, accuracy, and ease of use. Suitable for surface and feature measurements, even on reflective or multi-material surfaces, the scanner extends the capabilities of a CMM with the ability to digitize parts quickly. High-quality data is provided for insightful part-to-CAD comparison and reporting. The accuracy of the L100 is 2µm + L/350. The L100 is ideal for applications where high productivity and inspection accuracy are key. It is equipped with a top-quality Nikon glass lens custom-designed and optimized for laser scanning, as well as a high-definition camera capturing 2,000 non-interpolated points per line. The unit is perfectly suited for combined surface and feature measurements max 420,000 pts/sec[37].

1.6.15 The Sense

The iSense may be bowing out, but 3DSystem's Sense scanner, powered by the same software, is still going strong. Looking a bit like a space-age staple gun, the Sense is controlled through its proprietary software (PC only) and is connected to the computer by a cord. Cords on handheld scanners can require you to 'plan your route' when walking around the object you scanning. Like other handheld scanners mentioned here, the Sense is particularly vulnerable to how a user executes its trajectory and can quickly run into lost tracking issues. A benefit of this 3DSystem scanner is the large object size it's capable of capturing, substantiated by positive reports from users. The hardware setup in this scanner features two cameras and an infrared laser; the middle camera records the light pattern hitting the object to build the 3D geometry, and the other camera captures images used for texturing the final model. The market price is $399 [3].

1.7 Photogrammetry

Photogrammetry is a three-dimensional coordinate measuring technique that uses 2D photographs as the fundamental medium for metrology or measurement. The main principle used in photogrammetry is triangulation. By taking photographs from at least two different locations, so-called 'lines of sight' can be developed from each camera to a point to the object. These lines of sight, sometimes called rays owing to their optical nature, are mathematically intersected to produce the three-dimensional coordinates of the points of interest [5]. Photogrammetry is almost as old as photography itself. Since its development about 150 years ago, photogrammetry has moved from a purely analogue, optical-mechanical technique to analytical methods based on the computer-aided solution of mathematical algorithms and finally to digital or softcopy photogrammetry based on digital imagery and computer vision, which is devoid of any optomechanical hardware. Applications include the measuring of coordinates; the quantification of distances, heights, areas, and volumes; the preparation of topographic maps; and the generation of digital elevation models and orthophotographs [6].

1.7.1 History of photogrammetry

Astonishingly, the history of photogrammetry is nearly as old as that of photography itself, in the beginning, the major application of photogrammetry was limited to close range and architectural measurement rather than to topographical mapping. Leonardo da Vinci, one of the earlier explorers of photogrammetry, in 1492, started working with perspective and central projections with his invention of the Magic Lantern, but no evidence exists that he truly made a working model. The principles of perspective and projective geometry shape the root out of which photogrammetric theory is developed.

Aimé Laussedat, the first person, who used terrestrial photographs for topographic map compilation, in 1858, did an experiment with aerial photography supported by a string

of kites but deserted it after a few years. In 1862, the Science Academy in Madrid officially grants Laussedat's use of photography for mapping.

Paulo Ignazio Pietro Porro, an Italian geodesist and optical engineer invented the first tachometer in 1839. He, in 1847, improved the image quality of a lens system using three asymmetrical lens elements. He invented the panoramic camera in 1858 that was equipped with a sighting telescope, the compass, and a level followed by a photogoniometer in 1865. This development is notable in photogrammetry as its application in eliminating lens distortion. His main purpose was to look at the image with a telescope through the camera lens.

Meydenbauer, known for his architectural surveys using photogrammetry in 1867, designed a camera believing that the present cameras were not fit for photogrammetry. This was the first wide-angle lens used for mapping – 105o Pantoshop lens, also the topographic map of Freyburg, Germany, made using this camera.

In 1896, the first stereoscopic-plotting instrument called the Stereo- Planigraph invention by the surveyor General of the Dominion, Edouard Deville, also known as the "father of Canadian photogrammetry" was the first attempt to use stereo overlapping photos, but the intricacy of the instrument limited it to little use. Stereoscopy was developed from a Wheatstone Stereoscope for producing the stereo model in which, Deville used a tracer point to achieve the mapping. He was very accurate in the mapping of the Canadian Rocky Mountains.

In 1904, the U.S. Geological Survey started to use photogrammetry for topographic mapping. C. W. Wright and F. E. Wright took photos from the ground using a panoramic camera in their survey in Alaska. They used a commercial camera that was improved by adding level bubbles and internal scales within the camera.

In Germany, Eduard von Orel, 1908, invented the first stereo autograph which was important as its construction principles made close-range photogrammetry easier in mountainous areas. The operator traces elevation contours by stereo autograph directly.

In the early 1950s, Everett Merritt, a scientist at the Naval Photographic Interpretation Center in Washington, D.C developed analytical photogrammetry. He also developed analytical solutions for camera calibration, space resection, interior and exterior orientation, relative and absolute orientation of stereo pairs, and finally analytical control extension.

The invention of the computer in 1941 made significant developments in the field of photogrammetry after 1950.

The principles of modern multi-station analytical photogrammetry by matrix notation were developed by Dr Hellmut at the Ballistic Research Laboratory, Maryland in1953. The main principles of this development were "a thoroughly correct least-squares solution, and the simultaneous solution of any number of photographs, and a complete study of error propagation".

Digital photogrammetry was invented by one of the greatest scientists named Gilbert Louis Hobrough whose development in the field of digital photogrammetry was the beginning of a new era. His initial contributions in the field of photogrammetry intricated the development of an electronic dodging printer, which designed an airborne profile recorder adjoining by a radar system for measuring the one-foot accuracy level range from the aircraft to the ground and a reference barometer with equivalent accuracy [7]

1.7.2 Classification of photogrammetry

Two types of photogrammetry exist based on the location of the camera during photography. Firstly, aerial photogrammetry, and secondly, terrestrial photogrammetry [6].

1.7.3 Aerial Photogrammetry

Aerial photogrammetry is technically a subset of remote sensing that primarily involves visible light waves in the electromagnetic spectrum. There are some excellent uses in near-infrared applications as well. Aerial photography is perhaps the most widely used method for creating geographic databases in forestry and natural resource management. Interpretation techniques that involve geometry, trigonometry, optics, and familiarity with natural resources can allow us both to identify and estimate the size, length, or height of objects on the ground. Aerial photogrammetry requires the use of vertical aerial photographs (those where the axis of the camera was no more than 3° from vertical), and most often requires the use of stereo pairs (overlapping photos), although reasonable measurements can be made from single vertical aerial photographs if the scale of the photo can be determined. Many of the base maps used by natural resource management organizations were initially made with aerial photographs that were interpreted by natural resource managers. This information can be collected from the photographs using stereo compilers, which allow us to correct a large portion of the inherent error from sources of distortion and displacement. Alternatively, the detail associated with the interpreted photos can be transferred to maps using hand-drawing processes or traditional digitizing processes. Further, information about the camera and terrain can be combined in an analytical model that can compute the coordinates of features using softcopy (personal computer-based) photogrammetry techniques. In Aerial photogrammetry, we mount the camera on an aircraft pointing vertically toward the ground. [8].

1.7.4 Terrestrial Photogrammetry

Terrestrial photogrammetry deals with photographs taken with cameras located on the surface of the earth. The cameras could be either handheld or mounted on a tripod or pole. The main principle of this type of photogrammetry is that if the directions of the same objects are photographed from two different points on a baseline, their position can be measured by the intersection of the two rays from the same point concerning the baseline. Terrestrial photogrammetry is also known as close ranged photogrammetry as

the object and the camera is always within the 300m range. 3D models, measurements, and drawings are the main output of close-range photogrammetry [9].

1.7.5 Photogrammetry workflow

1.7.5.1 Take images

The first step of photogrammetry is to take multiple overlapping photos of the chosen object from various angles with common reference points in each photograph. For the best results, the overlapping photos are to be taken in a circle around the object sequentially. First, begin with a circle at a low angle, then do one more at a higher angle to capture the topmost surfaces. We should take at least 50% overlapping photos between each photo; 60-80% is ideal. It could be better to take a few extra photos of areas that hold important details.

There are a few important points to be considered during photography

- Make sure the object has a matt surface. Transparent objects like glass will not give acceptable results. It is better to convert reflective objects into matt using 3D scanning spray or a coat of paint.
- Depending on the software, minimum of 40-60 photos are enough for an object. But the quality of the output depends on the number of photos. The more you take photos, the more you get better results.
- For a better result, we should not move the object.
- Proper lighting is acceptable throughout the shoot.

1.7.5.2 Upload

The next step is to import the photos into the project library of photogrammetry software. For some software, it is crucial to examine the compatibility of the camera like focal length, and image sensor format. In the first step of the software pipeline, the photos will be examined to whether suitable for the photogrammetry process or not. During this process, a green or red icon may appear next to or on the top of the photos in the library. If a large portion of the photoset gets rejected, taking photos again would be a probable solution. Some photo editing software may come in handy. Software like meshroom requires an NVIDIA CUDA enable computer. Cloud-based software like Autodesk recap and Kiri engine also exist.

1.7.5.3 Creating a 3D model

Most of the computational part is carried out in the background by the photogrammetry software automatically. But a manual control programme with advanced features may improve the results.

a) Image Matching

The main purpose of this step is to get images that are looking at the same areas of the scene. For this, the image retrieval techniques are to be used to get images that share some content without the cost of revolving all features matches in detail. In simple, in this part, the software determines which photos are acceptable for further processing and search for overlapping areas in multiple images.

b) Feature Extraction

In this part, the software scours the photos for features that can be recognized across multiple images uniquely. Some professional toolkits use a very accurate method for this, named coded markers that even work on transparent, reflective, and other featureless surfaces. Most tools use the generic SFM (structure from motion) technique which searches for dense textures on objects, such as wood grain, texts, facial features, edge points, corners, and lines. Once all the features have been found, they are internally verified by geometric verification technique to sift out erroneous detections.

To ensure that the detected features fall onto the same scene point, the structure from the motion engine creates a transformation that maps feature points between images. It is a very complex set of algorithms based on projective geometry.

c) Triangulation

In this part, the software evaluates the 3D coordinates of the surface points based on the output of the previous steps. Lines of sight from the camera to the object are reconstructed resulting in what is known as the ray cloud. The intersections of all the rays determine the ultimate 3D coordinates of the object. To create a depth map, photogrammetry software looks at the lighting and texture of the scene. Advanced programmes use a technique named delighting to make the lit and shaded areas equal for more homogenous lighting across the complete surface of the model. It is also possible to reverse-calculate and cancel out ambient occlusion effects. While a realistically lit model is preferable for on-screen visualization purposes, a delit model is better for full-colour 3D printing. Then the *dense reconstruction* involving the depth map, and the *sparse reconstruction* that mapped out all visual features detected in the previous stages, are combined into a 3D mesh format such as FBX, OBJ, PLY, or STL.

The triangulation phase takes place automatically. The user may increase quality by elevating settings such as Track Length, number of Neighboring Cameras, and Maximum Points. Some photogrammetry programs also may allow the user to determine the number of triangles present in the 3D mesh object, affecting file size and ease of post-processing. Many photogrammetry software tools use different machine learning techniques to classify detected objects such as foliage, buildings, and vehicles. They can separate moving background objects such as birds and pedestrians, and establish enhanced shape data based on additional information like foreground silhouettes, reflectance, and irradiance. Thin shapes such as steel frameworks and power lines can automatically be recreated in 3D using so-called catenary curve fitting algorithms.

d) Post-processing

This is the easiest part of the photogrammetry process. The actual work starts when the 3D mesh model has been generated in the previous steps. There are usually floating artefacts, background noise, holes, and irregularities in the 3D mesh to be cleaned up. The object also needs to reorientate and rescale, which is done quite arbitrarily by photogrammetry software [9].

Some software may have in-built post-editing tools, such as Autodesk recap pro. otherwise, we may use Meshlab for necessary file conversations and MeshMixer for cleaning up, repairing, remeshing, and resculpting.

After this part is completed and the file is saved into STL format, the object is ready for 3D printing.

1.7.6 Photogrammetric Products

Photogrammetric systems give 3D object coordinates obtained from image measurements. Out of these, further elements and dimensions can be obtained, for example, areas, distances, lines, and surface definitions, also quality information including comparisons against design and machine control data. Without a clear calculation of point coordinates, the determination of geometric elements such as straight lines, planes, and cylinders is also obtainable. Also, the recorded image is an objective data store that documents the state of the object during recording. The visual data may be provided as accurate camera images, orthophotos, or graphical overlays.

1.7.7 Applications of photogrammetry

Photogrammetry can be used in numerous fields such as engineering, medicine, architecture, manufacturing, etc.

One of the best uses of photogrammetry is creating maps from aerial photos. Other uses of photogrammetry are given below:

1) By photogrammetry, we can accurately measure any image. When building a complex structure, it is extremely crucial to have precise measurements of everything. The planning and the execution should be flawless and due to this reason, photogrammetry is used. By using the images from drones, engineers may estimate the sites of construction accurately which confirms that everything runs efficiently without any difficulty. If a client wants to see the progress of the work, Photogrammetry is used to produce perspective images and 3D renderings which helps in evaluating the present work [10].
2) Photogrammetry plays a crucial role in film and entertainment. In recent times, filmmakers have started to deeply count on photogrammetry for 3D modelling and exact measurements that are essential for world-building for games and movies. photogrammetry has started to play a crucial role in countless CGI movies. The 3D modelling of photogrammetry may help in bringing the planned

virtual worlds like cities and other historical places with precise dimensions [10].

3) It is better to know all the details while solving a case is immensely vital and photogrammetry has a significant role in the crime investigation. Photogrammetry helps in documenting the accurate measurements of the scenes of crime while presenting the case before the court [10].
4) Land surveying is a method that uses science, measurements, and technologies to ascertain the surface of the earth. It uses photogrammetry to take true images of things such as landmasses. It also uses photogrammetry to get correct measurements of a specific object [10].

1.7.8 Accuracy of photogrammetry

The accuracy of photogrammetry mainly depends upon various factors such as:

I. Image resolution
II. Camera calibration
III. Angels
IV. Photo orientation quality

I. Image resolution

The higher the resolution of the images, the better chance of getting high accuracy as each item in the photos accurately can be located.

II. Camera calibration

It is the technique of determining the camera's lens distortion, focal length, format size, camera sensor, and primary point. We can get the best results by using a well-calibrated camera. If the cameras do not calibrate well due to fish eye lenses and the cameras are unstable, the accuracy will be lower. We will use a high-quality lens and stable camera for the best results.

III. Angels

Points and objects that appear only on photographs with extremely low subtended angles have much lesser accuracy than points on photos that are closer to 90 degrees apart. Making sure the camera positions have a good spread will give the best results. You can easily imagine that the accuracy of photogrammetry depends upon the angle between the rays of light. The smaller this angle, the less will be the accuracy.

IV. Photo orientation quality

During processing, photogrammetry software determines the location and angle of the camera for each photo. If the number of well-positioned points increases, the orientation quality improves as the points cover a greater proportion of the photograph area [11].

1.8 Literature reviews on photogrammetry

S.N Lane (2000) [12] reviews the progress that is being achieved by fluvial geomorphologists in making use of digital photogrammetry for river channel research. Fluvial geomorphology is first placed in a basic historical context from which the failure to make full use of the potential of photogrammetry is noted. He reviews how fluvial geomorphologists are now using photogrammetry, recognizing that the development of digital approaches has made photogrammetry a more cost-effective tool and introduced a range of new research questions. The main objective of this paper is to demonstrate the importance of these questions and to illustrate some of how they are being addressed.

Ayse Gulcin Kucukkaya (2004) [13] investigated the use of Photogrammetry and Remote Sensing in Archeology with the support of documents of the Fifth World Archeology Congress (WAC5) 2003, Session of "Remote Sensing for Archeology". Remotely sensed aerial and satellite imagery, alone or in conjunction with ground-based sensors, is a valuable tool for the characterization of the archaeological landscape and location of underground structures. Surface features caused by historic sites underground can be recorded with colour infrared film and digital multi-spectral, hyper-spectral, and synthetic aperture radar imagery.

The remote sensing and photogrammetric analysis of the ground in archaeological sites have obvious advantages compared with other older ones. It can detect the archaeological features not visible by the ground-based observer and these contact-less observations can be conducted without a visit to the site being investigated. The data obtained in these observations can be used also for geological and climatological purposes.

P.Ariasa, J.Herráez, H.Lorenzo,C.Ordóñeza (2005) [14] deals with the conservation of monumental buildings. Several methods used for architectonic documentation are analyzed in this study. Computer methods and close-range photogrammetry are proposed as the preventive method which allows for the detection, measurement, and tracking of the temporal evolution of some structural problems detected and also assesses the degree of conservation of the materials employed. A group of monuments belonging to the Spanish historical heritage is analyzed. A wire-frame model and a photo-realistic textured model were used to carry out the analysis. A detailed analysis of one of the building's parts and the numeric values obtained enable estimating the stresses undergone by any particular building. Thus, it will be possible to establish the collapsing risks of the monumental group analyzed. This information obtained using photogrammetric techniques will be particularly useful in the pre-processing phase of any finite element analysis since it can be used for establishing 3D geometries and help in choosing the type of element used. This way the obtained results will be more accurate, particularly where complex geometries are concerned. Finally, the selection and visualization of the results in the post-process phase will be more reliable, because data such as the principal stresses, the direction of the axis, etc. will be perfectly georeferenced about perfectly known directions.

De-hai Zhang, Liang Jin, Cheng Guo, and Zhi-xin Chen (2010) [15] developed a digital photogrammetry measurement system (XJTUDP) based on a close-range industry. Studies are carried out on key technologies of a photogrammetry measurement system, such as the high accuracy measurement method of a marker point centre based on a fitting subpixel edge, coded point desi,gn, and coded point autodetection, calibration of a digital camera, and automatic image point matching algorithms. The 3-D coordinates of object points are reconstructed using colinear equations, image orientation based on coplanarity equations, direct linear transformation solution, outer polar-line constraints, 3-D reconstruction, and a bundle adjustment solution. Through the use of circular coded points, the newly developed measurement system first locates the positions of the camera automatically. Matching and reconstruction of the uncoded points are resolved using the outer polar-line geometry of multiple positions of the camera. The normal vector of the marker points is used to eliminate the error caused by the thickness of the marker points. XJTUDP and TRITOP systems are tested based on VDI/VDE2634 guidelines, respectively. Results show that their precision is less than 0.1 mm/m. The measurement results of a large-scale waterwheel blade by XJTUDP show that this photogrammetry system can be applied to industrial measurements.

Naci Yastikli (2007) [16] used digital close-range photogrammetry successfully for the documentation of cultural heritage. This new method offers us new opportunities such as automatic orientation and measurement procedures, generation of 3D vector data, digital ortho-image, and digital surface model. Terrestrial laser scanning is another technology that in recent years has become increasingly popular for documentation which provides very dense 3D points on an object's surface with high accuracy. In addition, the 3D model and digital ortho-image can be easily generated using generated 3D point clouds and recorded digital images.

In this paper, methods in digital photogrammetry and terrestrial laser scanning are investigated for documentation of cultural heritage, particularly historic buildings. The most suitable approaches for documentation procedures from the data acquisition to the final product using monoscopic multi-image evaluation, stereo digital photogrammetry, and TOF terrestrial laser scanning are investigated with the help of three experiments. The results of the experiments showed that the new methods in digital photogrammetry and terrestrial laser scanning can be used successfully for cultural heritage documentation, which has very complex geometry and irregular shape. Also, this investigation has demonstrated that the whole documentation process including data acquisition, data processing, and final product can be carried out in a digital environment with the help of the automated procedures and digital aids that can be provided. The assignment of RGB colour value to the scanned 3D points and generation of meshes, textures, and ortho-images can be achieved automatically with the combined use of the terrestrial laser scanner and the digital camera.

Ruinian Jiang, David V.Jáuregui, and Kenneth R.White (2008) [17] presented a review on the basic development of close-range photogrammetry and briefly describes work related to bridge deformation and geometry measurement; structural test monitoring; and historic documentation. It is shown that early applications featured the use of metric cameras (specially designed for photogrammetry purposes), diffuse targets (non-retroreflective), stereoscopic photogrammetry network layout, and analogue analytical tools, which transformed over time to the use of non-metric cameras, retro-reflective targets, highly convergent network layout, and digital computerized analytical tools. Close-range photogrammetry has been found very useful in test monitoring due to its capability of measuring 3D deformation and behaviour up to the failure of bridge elements, which makes it very useful in torsion, shear, axial, and bending experiments. Close-range photogrammetry has also been found in historic bridge documentation and rehabilitation. They concluded that close-range photogrammetry is a powerful measurement technique that can provide unique solutions for broad and diverse bridge engineering applications.

Clive S.Fraser and Simon Cronk (2009) [18] presented a hybrid measurement approach that involves fully automatic network orientation with targets, while at the same time supporting follow-up semi-automatic and manual operations such as feature point and line extraction and surface measurement via image matching. The topics discussed include camera calibration, the metric exploitation of colour attributes, issues related to image point correspondence determination, operator-assisted feature measurement, and surface extraction. All are important to the practical realization of the hybrid measurement approach. Close-range photogrammetry employing consumer-grade cameras displays a good deal of presently unrealized potential for a broader base of measurement applications. The obvious prerequisites for wider usage are higher levels of process automation and greater measurement flexibility. This paper has described how the concept of hybrid measurement utilizing fully automatic network orientation with semi-automatic operator-assisted extraction of features of interest, be they unsignalized points, polylines, or surfaces, can be realized in practice. However, considerable research and development remain if the ‘holy grail’ goal of fully automatic multi-image orientation and marker-less object reconstruction is to be achieved without the use of coded targets and operator intervention in the surface extraction process.

Muammer Ozbek, Daniel J.Rixen, Oliver Erne, and Gunter Sanow (2010) [19] proposed photogrammetry to be a promising and cost-efficient alternative for monitoring the dynamic behaviour of wind turbines. The pros and cons of utilizing this measurement technique for several applications such as dynamic testing or health monitoring of large wind turbines are discussed by presenting the results of the infield tests performed on a 2.5 MW - 80 m diameter - wind turbine. Within the scope of the work, the 3D dynamic response of the rotor is captured at 33 different locations simultaneously by using 4 CCD (charge-coupled device) cameras while the turbine is rotating. Initial results show that the deformations on the turbine can be measured with an average accuracy of 25 mm from a measurement distance of 220 m. Preliminary analyses of the measurements also show that some of the important turbine modes can be identified from photogrammetric measurement data. Based on the results of the analyses reported in this paper, it can be concluded that the random component of the

coordinate measurement error is in the range of 5 mm or 1/16,000 of the field of view. The accuracy can be considered high and even improved further by using higher resolution cameras. The maximum value of the systematic error was found to be of the order of 30 mm in their calculations, the maximum being found for the outermost markers. Since the random error component is usually in the range of 5 mm, independent of the marker location, the maximum overall error could reach 35 mm for the tip marker. However, more sophisticated camera calibration, data processing, and comparison techniques can further reduce systematic error.

Thomas Luhmann (2010) [20] summarized recent developments and applications of digital photogrammetry in industrial measurement. Industrial photogrammetry covers a wide field of different practical challenges in terms of specified accuracy, measurement speed, automation, process integration, cost-performance ratio, sensor integration, and analysis. On-line and off-line systems are available, offering general-purpose systems on the one hand and specific turnkey systems for individual measurement tasks on the other. Verification of accuracy and traceability to standard units concerning national and international standards is inevitable in industrial practice. System solutions can be divided into the measurement of discrete points, deformations and motions, 6DOF parameters, 3D contours, and 3D surfaces. Recent and future developments concentrate on higher dynamic applications, integration of systems into production chains, multi-sensor solutions, and still higher accuracy and lower costs. He provided an overview of the state-of-the-art in industrial photogrammetry. The field can be characterized by demanding requirements in accuracy, price-performance ratio, level of automation, reliability, mobility, and flexibility. Photogrammetric systems compete with alternative solutions (e.g laser trackers and CMMs), but also provide unique advantageous features for non-contact measurement of points, surfaces, and structures. Industrial photogrammetry invariably employs imaging technology based on CCD and CMOS sensors, and off-the-shelf SLR, video, and high-speed cameras. For specific tasks, a limited number of specialized photogrammetric cameras exist that are optimized in terms of stability, image quality, accuracy, or speed. Cameras are used in offline and online applications and systems in a large number of industrial applications. While offline systems usually form the standard case of multi-image photogrammetry, online systems are either configured as tactile photogrammetric coordinate measurement systems, or as special purpose systems integrated into an external process. The calibration method and resulting accuracy are closely linked. The highest accuracies can be achieved with high-resolution sensors, multi-image configurations, targeted object points, and self-calibrating bundle adjustment. A precision of 5–10 ppm is readily achievable, while some accuracy figures may well be lower, for example, 20 ppm in terms of length measurement errors.

M.J.Westoby, J.Brasington, N.F.Glassera, M.J.Hambreya J.M.Reynolds (2012) [21] outlined a revolutionary, low-cost, user-friendly photogrammetric technique for obtaining high-resolution datasets at a range of scales, termed ‘Structure-from-Motion’ (SfM). Traditional softcopy photogrammetric methods require the 3-D location and pose of the camera(s), or the 3-D location of ground control points to be known to facilitate scene triangulation and reconstruction. In contrast, the SfM method solves the camera pose and scene geometry simultaneously and automatically, using a highly

redundant bundle adjustment based on matching features in multiple overlapping, offset images. As an initial appraisal of the technique, an SfM-derived DEM is compared directly with a similar model obtained using terrestrial laser scanning. This intercomparison reveals that decimetre-scale vertical accuracy can be achieved using SfM even for sites with a complex topography and a range of land covers. Example applications of SfM are presented for three contrasting landforms across a range of scales including; an exposed rocky coastal cliff; a breached moraine-dam complex; and a glacially-sculpted bedrock ridge. The SfM technique represents a major advancement in the field of photogrammetry for geoscience applications. Their results and experiences indicate that SfM is an inexpensive, effective, and flexible approach to capturing complex topography.

Armin Gruen (2010) [22] developed image matching techniques in photogrammetry and reviewed the results of some empirical accuracy studies and also provided a critical account of some of the problems of image matching. Although automated approaches have quite several advantages, the quality of the results is still not satisfactory and, in some cases, far from acceptable. Even with the most advanced techniques, it is not yet possible to achieve the quality of results that a human operator can produce. There is an urgent need for further improvements and innovations, be it through more powerful multi-sensory approaches, thereby enlarging the information spectrum, and/or through advancements in image understanding algorithms, thus coming closer to human capabilities of reading and understanding image content. The development of image matching in photogrammetry has been described chrono-logically. While the original approaches to image matching were derived from signal processing and image transfer requirements, specific models trying to consider the photogrammetric imaging and network aspects were introduced later. The underlying models for matching became more complex over time. With the advent of digital techniques, there was no longer any actual limit to the refinement of models but computing time considerations became critical issues. This is where the research stands today. Even though the matching problem has not yet been solved in general terms, quite refined models are available, with millions of match points produced per stereo model. Least squares matching can be used in many different modes and variations. As such, it provides for an algorithmic framework that is highly adaptive to various types of image content, network structures, processing requirements, and accuracy expectations. It has also been demonstrated in the past that least-squares matching allows exploitation of the full accuracy potential of images and systems. It provides for a measurement accuracy that goes way beyond the capabilities of a human operator.

M.Lato, J.Kemeny, R.M.Harrap, G.Bevand (2013) [23] proposed an idea of how different sensors and processing workflows are performed by LiDAR and photogrammetry. Two principles must be established to move across-the-board comparisons of remote rock mass characterization forward: (i) establishment of accessible, documented test sites, and (ii) test databases that are accessible to all. They proposed the establishment of several key sites for equipment tests, including already-studied areas in Europe and North America, as well as an open approach to adding sites and related data to the collection. Site descriptions must include detailed local geology, photographs, LiDAR and/or photogrammetry datasets, and access notes. Second, they

described and provided a prototype data repository for storing this information, and in particular for providing open access to benchmark data in the future. This initiative will allow for meaningful comparisons of sensors and algorithms and specifically will support better methodologies for benchmarking rock mass data in the geosciences. The idea proposed in this paper, and executed through the RockBench website, is to enable researchers and practising engineers in the field of remote imaging and engineering geology to test innovative algorithms for the mapping of geological features using open-source data. This will facilitate the benchmarking of results and comparability of algorithms, and hopefully, spur development in the field. The authors of this paper represent practitioners and developers; application specialists and theoretical scientists; LiDAR and photogrammetry experts; together combined their ideas to enable the comparative development of data processing algorithms.

M.Uysal, A.S.Toprak, N.Polata (2015) [24] evaluated the performance of cameras integrated UAV for geomatic applications by the way of Digital Elevation Model (DEM) generation in a small area (approximately 5 ha). For this purpose, 27 ground control points are surveyed with RTK, and 200 photos were captured with Canon EOS M. Over 26 million georeferenced points were used in the DEM generation process. The accuracy of the DEM was evaluated with 30 checkpoints and obtained 6.62 cm overall vertical accuracy from an altitude of 60 m.

Outcomes of the study show that the data derived from UAV Photogrammetry have adequate accuracy very much like RTK GPS data. So it is possible to use the UAV Photogrammetry data for map production, surveying, and some other engineering applications with the advantages of low-cost, time conservation, and minimum fieldwork.

J.A.Gonçalves, R.Henrique (2015) [25] analyzed the use of unmanned aerial vehicles (UAV) to map and monitor dunes and beaches. A very light plane equipped with a very cheap, non-metric camera was used to acquire images with ground resolutions better than 5 cm. The Agisoft Photoscan software was used to orientate the images, extract point clouds, build a digital surface model and produce orthoimage mosaics. The processing, which includes automatic aerial triangulation with camera calibration and subsequent model generation, was mostly automated. To achieve the best positional accuracy for the whole process, signalized ground control points were surveyed with a differential GPS receiver. Two very sensitive test areas on the Portuguese northwest coast were analyzed. Detailed DSMs were obtained with 10 cm grid spacing and vertical accuracy (RMS) ranging from 3.5 to 5.0 cm, which is very similar to the image ground resolution (3.2–4.5 cm). Where possible to assess, the planimetric accuracy of the orthoimage mosaics was found to be subpixel. Within the regular coastal monitoring program being carried out in the region, UAVs can replace many of the conventional flights, with considerable gains in the cost of the data acquisition and without any loss in the quality of topographic and aerial imagery data.

Birutė Ruzgienė and Tautvydas Berteška (2015) [26] reported investigations of how several GCPs used for UAV image transformation influence the mapping results. The demand for such investigations arises because the flight paths with a fixed-wing UAV

have a general form, in contrast to classical paths which are pricewise straight lines, as well as the flight significantly depends on weather conditions (especially on the wind) and the platform, shows considerable tilt because of its lightweight. The results of the DSM accuracy investigation demonstrate the quality of UAV Photogrammetry products with the use of an appropriate number of GCPs.

UAV Photogrammetry is a new valuable tool and provides low-cost small area, prompt data collection applicable for immediate image processing. The autopilot system guarantees a correct flight path and auto-controlled camera trigger. The interest in UAV systems' great potential for digital photogrammetry application is rising rapidly.

The UAV flight strips over the experimental area were generated as not straight patches as requires traditional aerial photogrammetry, the fly had a dependence on wind and vehicle was under a considerable tilt, and geodetic coordinates of each image projection centre were available with not high accuracy, i.e. of about 2 m. Because of such factors, upraises the demand for checking the correctness of photogrammetric production elaborated from UAV images.

The software Pix4D, used for experimental image processing, calculates initial and optimized values of interior image orientation parameters, here results show significant values of radial distortion – up to 45 μm.

The analysis of two mapping products (vector data onto orthophoto) shows significant distortions (even up to 3 m), in the case when UAV image rectification was performed only with PCCs (not using GCPs). Decreasing the number of GCPs from ten to well distributed five points, the features discrepancies are negligible.

DSM accuracy investigation in consideration with geodetic measurements of checkpoints shows, that when used only PCPs, estimators of accuracy (RMSE and StD) for the height points reach values up to 2 m. This confirms that the received data is suitable for small-scale mapping.

For the DSM, when images were processed with ten and five ground control points, the average RMSE and StD values are respectively: 0.064 m and 0.078 m. Therefore, processing the UAV images, gained with a high-resolution digital camera, when flying height is about 150 m and images are overlapped by more than 4 images, the DSM accuracy is of the required accuracy level (not exceeding the limitation of 25 cm) when for image transformation use the optimal number of GCPs – up to five. This proves a high accuracy of point height measurement applying the UAV Photogrammetry method, actually when the configuration of flight strips is not traditional.

Satoshi Nishiyama, Nao Minakata, Teruyuki Kikuchi, and Takao Yano (2015) [27] reported on the development of a novel automatic system for monitoring, updating, and controlling construction site activities in real-time. The proposed system seeks to harness advances in close-range photogrammetry to deliver an original approach that is capable of continuous monitoring of construction activities, with progress status

determined, at any given time, throughout the construction lifecycle. The proposed approach has the potential to identify any deviation from planned construction schedules, so prompt action can be taken because of an automatic notification system, which informs decision-makers via emails and SMS. This system was rigorously tested in a real-life case study of an in-progress construction site. The findings revealed that the proposed system achieved a significantly high level of accuracy and automation, and was relatively cheap and easier to operate. They reported the development of state of an art automated close-range photogrammetry-based approach for monitoring and controlling construction site activities. The case study demonstrated that the proposed system was novel and highly rigorous in automatically monitoring, analyzing, updating, and notifying the progress status of decision-makers. In particular, the system succeeded in instantly detecting any discrepancies from the as-planned schedule to provide various stakeholders with accurate and timely feedback. Thanks to this system, horizontal accuracy of 100% were achieved, while vertical accuracy exceeded 99.4%.

Once cameras are installed and programmed, the system does not require any expertise or manual intervention. Above all, the system is easy to use and much cheaper to operate. In addition, it can be used for any outdoor construction project. The progress status can be obtained anytime and anywhere.

Thomas Luhmann, Clive Fraser, and Hans-Gerd Maas (2016) [28] reviewed aspects of sensor modelling and photogrammetric calibration, with attention being focused on techniques of automated self-calibration. Following an initial overview of the history and the state of the art, selected topics of current interest within calibration for close-range photogrammetry are addressed. These include sensor modelling, with standard, extended and generic calibration models being summarised, along with non-traditional camera systems. Self-calibration via both targeted planar arrays and targetless scenes amenable to SfM-based exterior orientation is then discussed, after which aspects of calibration and measurement accuracy are covered. Whereas camera self-calibration is largely a mature technology, there is always scope for additional research to enhance the models and processes employed with the many camera systems nowadays utilized in close-range photogrammetry. Camera calibration has traditionally been and continues to be the single most significant factor determining the accuracy potential, and to a large extent also the reliability of close-range photogrammetric measurement. For much of the present era of digital photogrammetry, the well-known ‘standard’ physical calibration model attributable to Brown (1971) has served metric purposes for consumer-grade and professional photogrammetric cameras alike, and this model is yet to be found wanting in practical measurement applications, even at high accuracy tolerances. Moreover, self-calibration is now a fully automatic process and it is suited to both targeted and targetless objects and scenes. Notwithstanding these developments, the increasing application of non-traditional imaging systems and the desire to further develop and enhance calibration models will mean that metric camera calibration will continue as a topic of research interest in close-range photogrammetry.

Janowski Artur, Nagrodzka Godycka, and Ziolkowski Patryk (2016) [29] showed a potential spectrum of use for Terrestrial Laser Scanning (TLS) and photogrammetry in the diagnostics of reinforced concrete elements. Based on modes of failure analysis of

reinforced concrete beam authors describe downsides and advantages of adaptation of terrestrial laser scanning to this purpose, moreover reveal under which condition this technology might be used. Research studies were conducted by the Faculty of Civil and Environmental Engineering at the Gdansk University of Technology. An experiment involved bending the reinforced concrete beam, the process was registered by the terrestrial laser scanner. The reinforced concrete beam was deliberately overloaded and eventually failed by shear. The whole failure process was traced and recorded by scanner Leica Scan Station C10 and verified by synchronous photographic registration supported by digital photogrammetry methods. Obtained data were post-processed in Leica Cyclone (dedicated software) and MeshLab (program on GPL license). The main goal of this paper is to prove the effectiveness of TLS in the diagnostics of reinforced concrete elements. They propose a few methods and procedures to virtually reconstruct the failure process, measure geometry and assess the condition of the structure.

B.Kršák, P.Blišťan, A. Pauliková, P.Puškárová (2016) [30] analyzed the accuracy of the digital elevation model (DEM) obtained using low-cost UAV photogrammetry. The surface mine Jastrabá (Slovakia) was chosen as the test area. The mine has a morphologically dissected surface and is thus suitable for verifying the use of UAV photogrammetry to capture fairly intricate details on the surface. The research, which has been carried out, showed that the model created from photogrammetric data from the UAV achieves the accuracy required by current national legislation. From the selection of the test consisting of 237 points, only 3 points failed the conditions for the accuracy of the detailed points. These results indicate that the combination of a low-cost UAV and a digital camera may be used as a viable alternative for the collection of data to document surface structures and form 3D models formed from this data. The use of UAV in a photogrammetric survey of the mine brings new opportunities for the creation of documentation because with this technology we can measure the entire surface in detail, create orthophoto maps of the entire area, and document inaccessible parts of the area such as sludge dumps, and steep slopes.

Javad Baqersad, Peyman Poozesh, Christopher Niezrecki, and Peter Avitabile (2017) [31] reviewed the most current trends in the photogrammetry technique (point tracking, digital image correlation, and target-less approaches) and compares the applications of photogrammetry to other measurement techniques used in structural dynamics (e.g. laser Doppler vibrometry and interferometry techniques). The paper does not present the theoretical background of the optical techniques, but instead presents the general principles of each approach and highlights the novel structural dynamic measurement concepts and applications that are enhanced by utilizing optical techniques.

Jacob A. Morgan, Daniel J. Brogan, and Peter A. Nelson (2017) [32] reviewed how structure-from-Motion (SfM) photogrammetry become widely used for topographic data collection in field and laboratory studies. However, the relative performance of SfM against other methods of topographic measurement in a laboratory flume environment has not been systematically evaluated, and there is a general lack of guidelines for SfM application in flume settings. As the use of SfM in laboratory flume settings becomes more widespread, it is increasingly critical to develop an understanding of how to acquire and process SfM data for a given flume size and

sediment characteristics. In this study, they: (1) compare the resolution and accuracy of SfM topographic measurements to terrestrial laser scanning (TLS) measurements in laboratory flumes of varying physical dimensions containing sediments of varying grain sizes; (2) explore the effects of different image acquisition protocols and data processing methods on the resolution and accuracy of topographic data derived from SfM techniques; and (3) provide general guidance for image acquisition and processing for SfM applications in laboratory flumes. To investigate the effects of flume size, sediment size, and photo overlap on the density and accuracy of SfM data, we collected topographic data using both TLS and SfM in five flumes with widths ranging from 0.22 to 6.71 m, lengths ranging from 9.14 to 30.48 m, and median sediment sizes ranging from 0.2 to 31 mm. Acquisition time, image overlap, point density, elevation data, and computed roughness parameters were compared to evaluate the performance of SfM against TLS. We also collected images of a pan of gravel where we varied the distance and angle between the camera and sediment to explore how photo acquisition affects the ability to capture grain-scale microtopographic features in SfM-derived point clouds. A variety of image combinations and SfM software package settings were also investigated to determine optimal processing techniques. Results from this study suggest that SfM provides topographic data of similar accuracy to TLS, at higher resolution and lower cost. They found that about 100pixels per grain are required to resolve grain-scale topography. They suggest protocols for image acquisition and SfM software settings achieve the best results when using SfM in laboratory settings. In general, convergent imagery, taken from a higher angle, with at least several overlapping images for each desired point in the flume will result in an acceptable point cloud.

Hany Omar, Lamine Mahdjoubi, and Gamal Kheder (2018) [33] reported on the development of a novel automatic system for monitoring, updating, and controlling construction site activities in real-time. The proposed system seeks to harness advances in close-range photogrammetry to deliver an original approach that is capable of continuous monitoring of construction activities, with progress status determined, at any given time, throughout the construction lifecycle. The proposed approach has the potential to identify any deviation from planned construction schedules, so prompt action can be taken because of an automatic notification system, which informs decision-makers via emails and SMS. This system was rigorously tested in a real-life case study of an in-progress construction site. The findings revealed that the proposed system achieved a significantly high level of accuracy and automation, and was relatively cheap and easier to operate. This paper reported the development of state of an art automated close-range photogrammetry-based approach for monitoring and controlling construction site activities. The case study demonstrated that the proposed system was novel and highly rigorous in automatically monitoring, analyzing, updating, and notifying the progress status of decision-makers. In particular, the system succeeded in instantly detecting any discrepancies from the as-planned schedule to provide various stakeholders with accurate and timely feedback. Once cameras are installed and programmed, the system does not require any expertise or manual intervention. Above all, the system is easy to use and much cheaper to operate. In addition, it can be used for any outdoor construction project. The progress status can be obtained anytime and anywhere.

I. Colomina, P. Molina (2019) [34] discussed the evolution and state-of-the-art use of Unmanned Aerial Systems (UAS) in the field of Photogrammetry and Remote Sensing (PaRS). UAS, Remotely-Piloted Aerial Systems, Unmanned Aerial Vehicles, or simply, drones are a hot topic comprising a diverse array of aspects including technology, privacy rights, safety and regulations, and even war and peace. Modern photogrammetry and remote sensing identified the potential of UAS-sourced imagery more than thirty years ago. In the last five years, these two sister disciplines have developed technology and methods that challenge the current aeronautical regulatory framework and their traditional acquisition and processing methods. Naivety and ingenuity have combined off-the-shelf, low-cost equipment with sophisticated computer vision, robotics, and geomatic engineering. The results are cm-level resolution and accuracy products that can be generated even with cameras costing a few hundred euros. In this review article, following a brief historic background and regulatory status analysis, we review the recent unmanned aircraft, sensing, navigation, orientation, and general data processing developments for UAS photogrammetry and remote sensing with emphasis on the nano-micro-mini UAS segment.

Jakob Iglhaut, Jakob Iglhaut, and James O'Connor (2019) [35] presented that the adoption of Structure from Motion photogrammetry (SfM) is transforming the acquisition of three-dimensional (3D) remote sensing (RS) data in forestry. SfM photogrammetry enables surveys with little cost and technical expertise. They presented the theoretical principles and practical considerations of this technology and show the opportunities that SfM photogrammetry offers for forest practitioners and researchers. Their examples of key research indicate the successful application of SfM photogrammetry in forestry, in an operational context and research, delivering results that are comparable to LiDAR surveys. Reviewed studies have identified possibilities for the extraction of biophysical forest parameters from airborne and terrestrial SfM point clouds and derived 2D data in area-based approaches (ABA) and individual tree approaches. Additionally, increases in the spatial and spectral resolution of sensors available for SfM photogrammetry enable forest health assessment and monitoring. The presented research reveals that coherent 3D data and spectral information, as provided by the SfM workflow, promote opportunities to derive structural and physiological attributes at the individual tree crown (ITC) and stand levels.

Hashem Mohammad Khris (2021) [36] aimed to help archaeologists, museum curators, and technicians in understanding the principle of using photogrammetry and 3D scanner for museum archaeological objects in a practical way by presenting specific examples for both methods. Another purpose is to evaluate the performance offered by the photogrammetry and the three-dimensional (3D) scanner device, to provide a suitable solution to the different shapes and sizes of the archaeological objects. They used the camera Canon EOS 1300 D for photographing and Einscan Pro 2X Plus as a 3D scanning device for several years on different kinds of objects made of various materials, including ceramic, stone, glass, and metal. They showed that both approaches create 3D models with high resolution in easy and different ways.

1.9 Objective of Present Research

The main objectives of this project are:

1. To explore the possibility of implementation of reverse engineering using the photogrammetry technique
2. To compare the various software available for photogrammetry
3. To carry out 3D printing by photogrammetry technique and compare the performance of various 3D photogrammetry software
4. To measure and calculate the accuracy of photogrammetry

Chapter 2

2. Various Software Available For Photogrammetry

2.1 Autodesk ReCap Pro

Autodesk ReCap Pro is a reality capture software developed by Autodesk, letting designers and engineers capture accurate and detailed models of real-world assets. You can access advanced photogrammetry possibilities such as aerial photogrammetry and measure and edit point cloud data. Autodesk ReCap Pro has a wide range of tools for post-processing, allowing you to clean the unwanted objects to work more specifically on a precise object!

The price of this software is $USD 215 per year. But students can get this software free for one year by verifying their student identity cards [38].

System Requirements for Autodesk ReCap Pro: [39]

Minimum system specification	
Operating system	Windows 10 (64-bit)
CPU Type	2.0 GHz or faster 64-bit (x64) processor
Memory	4 GB system RAM
Display Card	OpenGL 3.1 capable graphics device with 256 MB graphics memory
Display Resolution	1280*1024 with true colour

System requirements for Autodesk ReCap Photo

Minimum system specifications	
Operating System	Microsoft Windows 10 (64-bit)
CPU Type	2.0 GHz or faster 64-bit (x64) processor
Memory	16GB RAM
Display Card	Video Nvidia GFX card with 4GB VRAM The graphics card must support DirectX 11

2.2 Kiri Engine App

Kiri Engine is a piece of software created to enable users to textured 3D scans from mobile devices and KIRI Innovations Science and Technology Inc's cloud services and customized for Apple and Android devices. It is used to 3D scan and digitalizes physical objects.

It is the most affordable photogrammetry app in the market. The price of this software is $USD 57 annually.

Advantages

1. The 3D model comes with textures, it looks so real when you put the model into an augmented reality application.
2. Sometimes size matters, this app provides low-poly options so the 3D model would always have the right size for the application.

Disadvantages

This app has only one disadvantage, it does not have any post-editing tools. we have to depend upon the other 3rd party applications for necessary file conversations and cleaning up, repairing, remeshing, and resculpting.

System requirements: Android version 7 and up [40].

2.3 AliceVision Meshroom

Meshroom is a free, open-source photogrammetry software that is based on the AliceVision framework.

System Requirements:

Hardware: To fully utilize Meshroom, an NVIDIA CUDA -enabled GPU is recommended. The binaries are built with CUDA-10 and are compatible with compute capability 3.0 to 7.5 without a supported NVIDIA GPU, only "Draft meshing" can be used for 3D reconstruction.

Operating system: Microsoft Windows 8 and up and Linux (Ubuntu)

Meshroom does not have any post-editing tools. We need some other software like Blender for post-processing [41].

2.4 Agisoft Metashape

Agisoft Metashape is professional software that performs photogrammetric processing of digital images for various applications, such as Geographic Information System applications, cultural heritage documentation, visual effects, production, as well as for indirect measurements of objects of various scales. Some important features enable Metashape to process various types of imagery (whether aerial or close-range), output a point cloud, measure distances, areas, and volumes, and generate 3D meshes that can then be exported to various popular formats. It is also possible to edit 4D models, which means entire scenes can be recorded in 3D and then manipulated on the software.

Two editions of the Agisoft Metashape license exist, the professional edition costs $3,499, and the standard one, $179 [42].

Advantages:

- Highly accurate and detailed Results.
- Fully automated and intuitive Workflow.

- GPU acceleration for faster processing.
- Easy sharing with PDF or fly-through video export and direct upload to online resources.
- Stereoscopic measurements for precise feature extraction.
- Agisoft Cloud for processing, visualization & sharing of the results. Reasonably powerful Standard edition for art projects.

System Requirements:

CPU: 32 vCPU (2.7 GHz Intel Xeon E5 2686 v4)

GPU: 2 x NVIDIA Tesla M60

RAM: 240 Gb

OS: Window, Linux (Ubuntu/ Debian)

2.5 PhotoModeler Technologies

More likely to be suited for CAD or CNC manufacturing than some of the other photogrammetry software solutions on the market, PhotoModeler offers exact measurements and models from photographs taken with an ordinary camera, just like the one you have on your smartphone. This is a cost-effective solution for accurate 2D or 3D measurement, as well as surveying, digitizing, reality capture, and more. Inside PhotoModeler, you can choose three different methods to generate the model you are trying to recreate. You can manually match common features between images, automatically generate a 3D model from coded targets, or generate point clouds from overlapping images. Three products exist, Standard, Premium, and Maintenance Agreements; price varies according to this and whether your license is permanent, renewable, or monthly.

The standard version costs USD 475 and the premium version costs USD 1255. This software only runs on Windows 7 and up.

2.6 Reality Capture

CapturingReality created the RealityCapture photogrammetry software that works with a wide variety of input media. It enables you to create virtual reality scenes, textured 3D meshes, orthographic projections, geo-referenced maps, and much more from images. It is also possible to work with laser scans on this software if you are looking for both options. The user interface is clean and modern, as well as intuitive for people who haven’t used this software before.

The company offers four different plans for its software, ranging from €19.90 to €15,000 for bigger business projects.

System Requirements:

- CPU: Decent i7/i9
- Geforce GTX 1060, 70 or 80,
- RAM: 16-32GB RAM.
- The GPU must support CUDA
- 64bit machine with at least 8GB of RAM
- 64bit Microsoft Windows version 7 / 8 / 8.1 / 10 or Windows Server version 2008+
- NVIDIA graphics card with CUDA 3.0+ capabilities and 1GB VRAM
- CUDA Toolkit 10.2, minimal driver version 441.22

2.7 Regard 3D

Regard3D is a free and open-source structure-from-motion program, that allows you to generate great 3D models from a series of photographs. This program is offering powerful tools and it might take you a while to master it. All the tutorials available on their website are really useful to get started. The software offers a comprehensive toolset for editing the point cloud, either with coloured vertices or a texture, before generating a 3D mesh.

Regard3D can be a little tricky for beginners to get to grips with, especially when using the advanced settings, but it's a good software for inexperienced users to get to grips with.

Regard3D can be run on various platforms, including Windows, Linux, and OS X.

2.8 3DF Zephyr

3DF Zephyr is a software solution by 3DFlow designed to be as user-friendly as possible. Some easy-to-use wizards explain processes and help you choose the right settings to help you generate 3D scans, so it's a great software for beginners.

This professional photogrammetry software can align photogrammetry data with laser scans, you can retain texture maps with increasing the accuracy of your model. Users can also benefit from a wide range of exporting options into many file formats. The process can be done automatically, or you can manually intervene if you want to work with your scan in CAD software.

There is a free version of 3DF Zephyr, but this is limited to 50 images for a 3D reconstruction. There are multiple licensing options for the paid version, with the price ranging from $175 to $4,576 depending on the features you want to have included.
While the free version is decent, the paid version offers a far more extensive range of advanced features, including multi-ICP registration, statistical analysis and reporting, a point cloud comparison tool, and the ability to control points, measurements, and volumes, to name just a few.

Minimum System Requirements:

- OS: Windows 10/8.1/8/7/Vista (64-bit)
- Processor: Dual Core 2.0GHz or equivalent processor
- Memory: 16GB System RAM
- Hard Disk Space: 10GB free HDD Space
- Video Card: Direct X 9.0c compliant NVIDIA video card with at least 1GB of RAM

2.9 Pix4D

Pix4D is professional photogrammetry and drone mapping software that provides a beginning-to-end photogrammetry solution, meaning that as well as generating point clouds, elevation maps and 3D meshes from imagery, it also assists in the capture of suitable images. Pix4D has developed a mobile photogrammetry app for iOS and Android, Pix4Dcapture, turning consumer drones into professional mapping tools. At the time of writing, the app supports DJI, Yuneec, and Parrot drones. The app controls the drone's flight path to ensure there's enough overlap between images for photogrammetric processing. Once the imagery is captured, it's processed in the Pix4D software where you can generate point clouds, elevation models, index maps, and orthomosaics. The software can be run on your desktop or the cloud. This software is best suited to applications such as agriculture, architecture, surveying, and construction. There are different versions suited to different applications; for example, Pix4Dmapper is the software for professional photogrammetry drone mapping, while Pix4Dfields is for field mapping and aerial crop analysis for digital farming. Pix4D is also an excellent tool for collaboration. You can share annotations, maps, and models via URLs, making it easy to bring team members onto a single project.

Prices range from $38 a month to $360 a month. For certain packages, you'll need to get a custom quote. There's a rich amount of support and training materials to help you use the software.

Minimum System Requirements:

- ❖ Windows 10, 64 bits (PC or Mac computers using Boot Camp). (Windows 11 is not supported yet)
- ❖ Any CPU (Intel i5/ i7/ Ryzen 7).
- ❖ Any GPU that is compatible with OpenGL 3.2. (Integrated graphics cards Intel HD 4000 or above).
- ❖ Small projects (under 100 images at 14 MP): 4 GB RAM, 10 GB HDD Free Space.

- Medium projects (between 100 and 500 images at 14 MP): 8 GB RAM, 20 GB HDD Free Space.
- Large projects (between 500 and 1000 images at 14 MP): 16 GB RAM, 40 GB HDD Free Space.
- Very Large projects (1000 -2000 images at 14 MP): 32 GB RAM, 80 GB HDD Free Space.

2.10 WebODM

This open-source photogrammetry software was released in 2017 by Open Drone Map, an ecosystem of solutions for collecting, analyzing, and displaying aerial data. WebODM uses aerial images from drones to produce point clouds, textured 3D photogrammetry models, digital elevation models, volume and area calculations, and geo-referenced maps.

This drone photogrammetry software has received many updates since its release and is now one of the most powerful, feature-rich free mapping software packages on the market. It's also highly configurable, so you may have to spend some time adjusting the modelling parameters to get the optimal result, but as free photogrammetry software goes it's certainly one of the best around once you've got the hang of it.

WebODM is almost completely free – there's a one-time fee of $57 for the installation if you don't want to have to download the source code and install it manually, though this is a small price to pay for high-quality photogrammetry software. You can use the software both on your desktop offline and on the cloud.

Minimum System Requirements:

For Windows

- Windows 8 or newer
- 64bit CPU with MMX, SSE, SSE2, SSE3, and SSSE3 instruction set support or higher 20 GB free disk space
- 4 GB RAM *

For macOS

- macOS 10.13 or newer. Apple Silicon (M1) is supported.
- Mac hardware must be a 2010 or newer model and support virtualization.
- 20 GB free disk space
- 4 GB RAM [42]

Chapter 3

3. Comparison of Autodesk ReCap Pro and Kiri Engine

In this experiment, the performance of two photogrammetry software Autodesk ReCap Pro and Kiri Engine app has been compared.

3.1 Equipment

- Fusion 360: Fusion 360 is a cloud-based 3D modelling, CAD, CAM, CAE, and PCB software platform for product design and manufacturing.
- Autodesk Recap Pro and Kiri Engine (Photogrammetry Software)
- Computer
- Ultimaker Cura 5.0.0
- Windows 10 Pro operating system for Autodesk Recap Pro
- Android 10 for Kiri Engine App
- FDM (Fused deposition modelling)
- PLA (Polylactic acid or polylactide)
- Infinix hot 10 Mobile with Android 10 OS and 16MP camera
- Object 1: A cube of 30mm*30mm*30mm dimensions
- Object 2: A cylinder of 40mm in diameter and 40mm in height
- Meshmixer Software: Autodesk meshmixer is a free software for creating and manipulating 3D files for 3D printing. Whether you need to clean up a 3D scan, do some 3D printing, or design an object, meshmixer can help.
- Digital Vernier calliper

3.2 FDM (FUSED DEPOSITION MODELLING)

In this experiment, a handmade FDM is used to obtain the 3D model. The x and z-axis movements are obtained by the extruder and the bed gives the Y-axis movement.

3.2.1 Key specifications of the FDM for this experiment

- Layer Height: 0.2mm
- Wall thickness: 0.8mm
- Infill density: 90%
- Printing temperature: 200°C
- Build plate temperature: 60°C
- Print Speed: 50mm/s

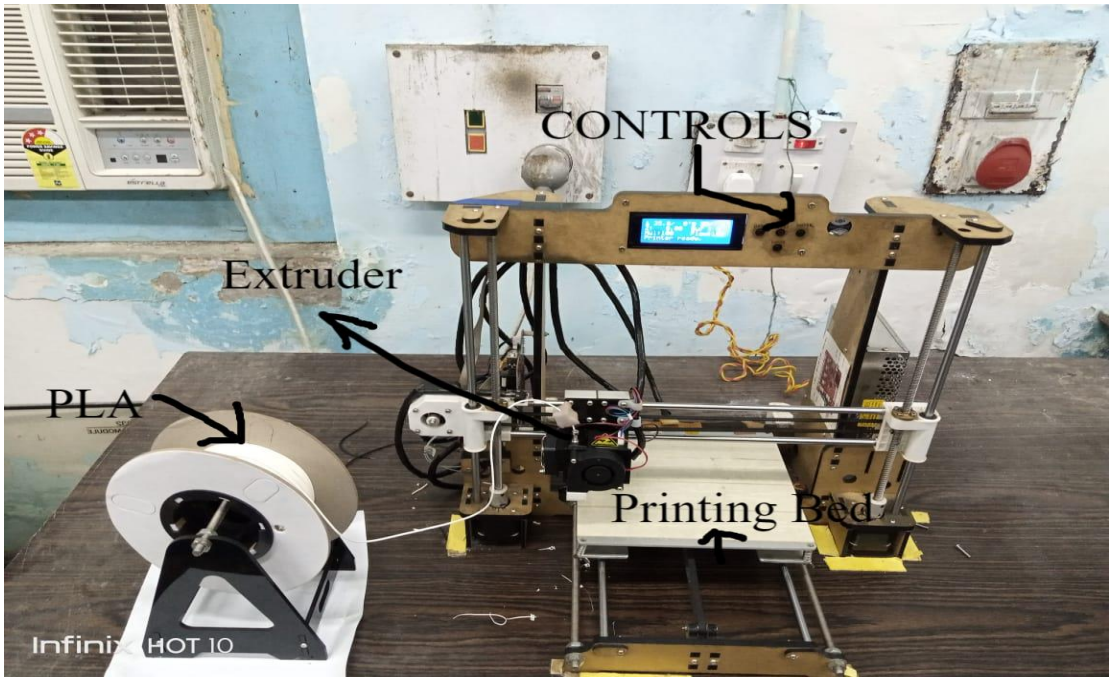

Figure 1: Photographic view of the FDM setup

3.2.2 Working Principle of the FDM

Fused deposition modelling (FDM) is an additive manufacturing technology commonly used for modelling, prototyping, and production applications.

The Fused Deposition Modelling (FDM) process constructs three-dimensional objects directly from 3D CAD data. A temperature-controlled head extrudes thermoplastic material layer by layer.

The FDM process starts with importing an STL file of a model into pre-processing software. This model is oriented and mathematically sliced into horizontal layers varying from +/- 0.127 - 0.254 mm in thickness. A support structure is created where needed, based on the part's position and geometry. After reviewing the path data and generating the toolpaths, the data is downloaded to the FDM machine.

The system operates in X, Y, and Z axes, drawing the model one layer at a time. This process is similar to how a hot glue gun extrudes melted beads of glue. The temperature-controlled extrusion head is fed with thermoplastic modelling material that is heated to a semi-liquid state. The head extrudes and directs the material with precision in ultrathin layers onto a fixtureless base. The result of the solidified material laminating to the preceding layer is a plastic 3D model built up one strand at a time. Once the part is completed the support columns are removed and the surface is finished.

Process:

FDM begins with a software process, developed by Stratasys, which processes an STL file (stereolithography file format) in minutes, mathematically slicing and orienting the model for the build process. If required, support structures are automatically generated. The machine dispenses two materials – one for the model and one for a disposable support structure.

The thermoplastics are liquefied and deposited by an extrusion head, which follows a tool path defined by the CAD file. The materials are deposited in layers as fine as 0.04 mm (0.0016") thick, and the part is built from the bottom up – one layer at a time. FDM works on an "additive" principle by laying down material in layers. A plastic filament or metal wire is unwound from a coil and supplies material to an extrusion nozzle which can turn the flow on and off. The nozzle is heated to melt the material and can be moved in both horizontal and vertical directions by a numerically controlled mechanism, directly controlled by computer-aided manufacturing (CAM) software package. The model or part is produced by extruding small beads of thermoplastic material to form layers as the material hardens immediately after extrusion from the nozzle. Stepper motors or servo motors are typically employed to move the extrusion head.

Several materials are available with different trade-offs between strength and temperature properties. As well as acrylonitrile butadiene styrene (ABS)polymer, polycarbonates, polycaprolactone, polyphenyl sulfones, and waxes. A "water-soluble" material can be used for making temporary supports while manufacturing is in progress, this soluble support material is quickly dissolved with specialized mechanical agitation equipment utilizing a precisely heated sodium hydroxide solution [43].

3.3 Equipment setup

Fusion 360 and Autodesk Recap pro were installed onto the computer and the Kiri Engine app was installed on the infinix hot 10 Mobile. FDM was also set up for printing.

3.4 Preparation of the actual cube for the experiment

A cube of 30mm*30mm*30mm dimensions was drawn in Fusion 360. A stereolithographic format (STL file format) was developed for the model drawn in Fusion 360. The STL file was then sliced in Ultimaker Cura and converted to a gcode file for 3D printing. It was then printed using FDM.

3.5 Preparation of the actual cylinder for the experiment

A cylinder of 40mm in diameter and 40mm in height was drawn in Fusion 360 and saved in STL format. The STL file was then sliced in Ultimaker Cura and scaled as x-axis, y-axis, and z-axis to 40mm respectively. Later it was 3D printed by FDM.

3.6 Autodesk Recap Pro Experiment 1

A total of 200 photos were taken around the cube in a circle. Then all the photos were imported into the Autodesk ReCap Pro for the photogrammetry process. Once the 3D model was generated, it was clean up by the "edit" tool of the Autodesk ReCap Pro software. The 3D model was sliced in Ultimaker Cura 5.0.0 and it was scaled as X-axis to 30mm, Y-axis to 29.9652, and Z-axis to 27.2817. The Y-axis and Z-axis were scaled automatically by the software. It was then printed by FDM as described earlier.

Figure 3: Photographic view of cube obtained by Photogrammetry using Autodesk Recap Pro

The width of all 4 sides of the cube generated by Autodesk Recap pro was measured using a digital vernier calliper at 3 different points.

All 4 faces were denoted as AB, CD, EF, GH

Table 1: Measurement data of AB, CD, EF, and GH are tabulated below.

Faces	Point 1	Point 2	Point 3	AVG	SDF
AB	29.08	28.58	28.87	28.84333	0.251064
CD	28.98	28.45	28.64	28.69	0.268514
EF	29.04	28.58	28.95	28.85667	0.24379
GH	29.01	28.45	28.84	28.76667	0.287112

All dimensions are in mm

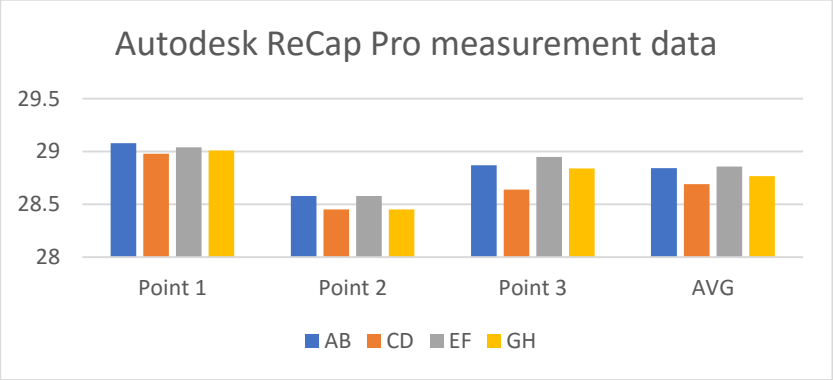

Figure 4: Bar Chart representation of Autodesk Recap Pro measurement data

(All dimensions are in mm)

The height of all 4 faces was measured using a digital vernier calliper at 3 different points. These 4 faces are denoted as IJ, KL, MN, and OP.

Table 2: Measurement data of IJ, KL, MN, and OP are tabulated below

Height	Point 1	Point 2	Point 3	AVG	SDV
IJ	27.11	27.32	27.44	27.29	0.167033
KL	27.55	27.41	27.38	27.44667	0.090738
MN	27.61	27.36	27.1	27.35667	0.255016
OP	27.42	27.35	27.47	27.41333	0.060277

All dimensions are in mm

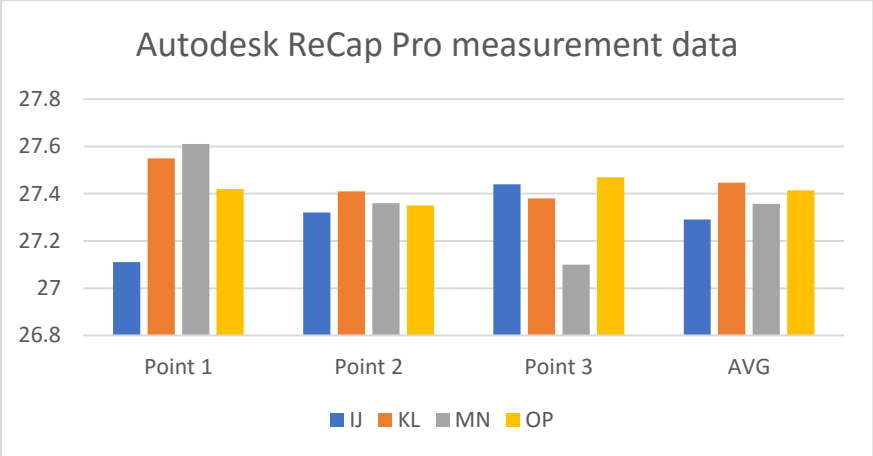

Figure 5: Bar chart representation of Autodesk ReCap Pro measurement data

(All dimensions are in mm)

The top two faces, ST, UV, and the bottom two faces denoted as WX, and YZ of the cube was also measured using a vernier calliper at 3 different points.

Table 3: Measurement data of ST, UV, WX, and YZ are tabulated below

Faces	Point 1	Point 2	Point 3	AVG	SDV
ST	28.98	28.93	28.97	28.96	0.026458
UV	28.93	28.8	29.03	28.92	0.115326
WX	28.94	28.82	28.97	28.91	0.079373
YZ	28.96	28.86	29.26	29.02667	0.208167

All dimensions are in mm

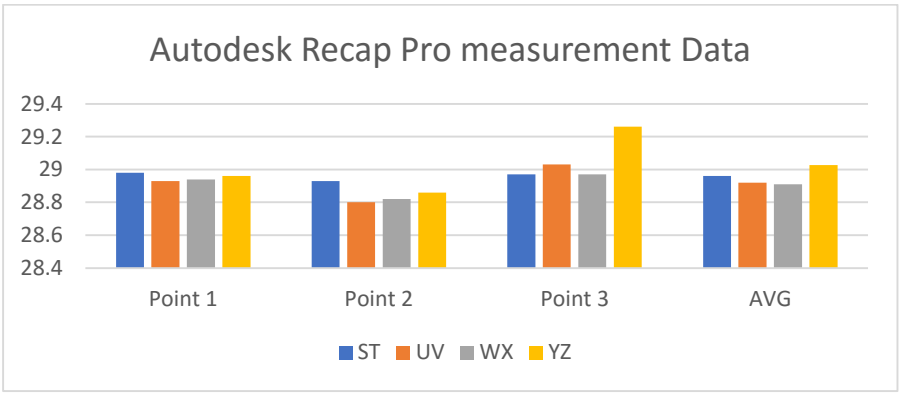

Figure 6: Bar chart representation of Autodesk ReCap measurement data

(All dimensions are in mm)

Also, measurement data of all the diagonals are tabulated below (All dimensions are in mm)

Diagonals	1-2	3-4	5-6	7-8	9-10	11-12	13-14	15-16	17-18
Value	39.15	38.92	39.10	38.81	39.10	39.07	39.04	39.09	39.49

Diagonals	19-20	21-22	23-24	15-18	14-20	10-18
Value	39.96	39.83	39.38	43.20	45.28	40.18

3.7 Autodesk ReCap Pro experiment 2

A total of 200 photos were taken around the cylinder in a circle. Then all the photos were imported into the Autodesk ReCap Pro for the photogrammetry process. Once the 3D model was generated, it was cleaned up by the "edit" tool of the Autodesk ReCap Pro software. The 3D model was sliced in Ultimaker Cura 5.0.0 and it was scaled as X-axis to 40mm, Y-axis to 39.9756, and Z-axis to 41.333. The Y-axis and Z-axis were scaled automatically by the software. It was then printed by FDM as described earlier.

Figure 7: Photographic view of cylinder obtained by photogrammetry using Autodesk Recap Pro

Table 4: The diameter of the cylinder at point 1,2,3 tabulated below (All dimensions are in mm)

Points	Diameter
1	41.43
2	40.63
3	40.40

Table 5: The height of the cylinder at three different points around the cylinder obtained by Autodesk ReCap Pro is tabulated below (All dimensions are in mm)

Points	Height
4-5	39.40
6-7	39.13
8-9	39.17

3.8 Kiri Engine Experiment 1

A total of 200 photos were taken around the cube in a circle. Then all the photos were imported into the Kiri Engine for the photogrammetry process. Once the 3D model was generated, it was clean up in the MeshMixer software. The 3D model was sliced in Ultimaker Cura 5.0.0 and it was scaled as X-axis to 30mm, Y-axis to 32.0344, and Z-axis to 30.9356. The Y-axis and Z-axis were scaled automatically by the software. It was then printed by FDM as described earlier.

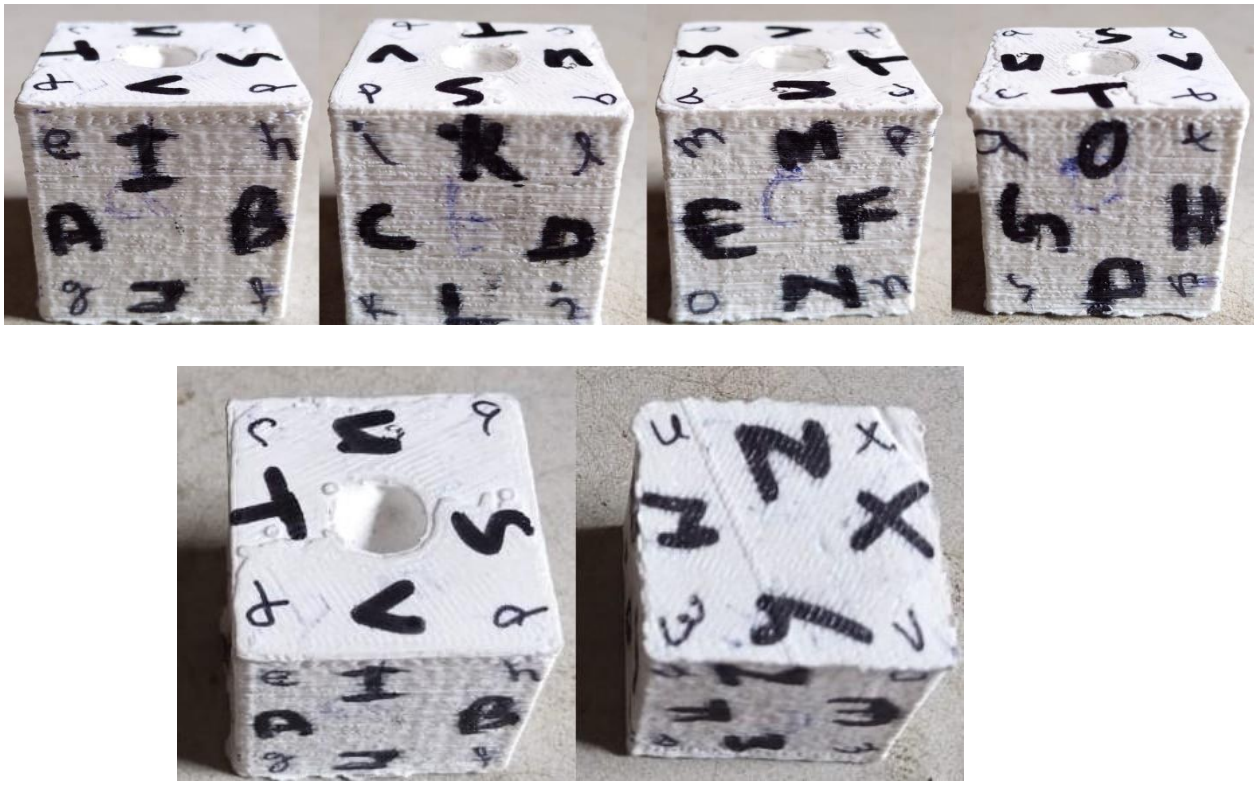

Figure 8: Photographic view of cube obtained by photogrammetry using Kiri Engine

Table 6: Measurement data of all the faces are tabulated below

Faces	Point 1	Point 2	Point 3	Average	STDEV
AB	31.38	30.89	31.72	31.33	0.417253
CD	31.58	30.84	31.81	31.41	0.506853
EF	31.04	30.99	31.39	31.14	0.217945
GH	31.55	30.87	31.66	31.36	0.427902
UV	31.49	31.69	32.07	31.75	0.294618
ST	31.62	31.51	31.51	31.54667	0.063509
WX	31.23	31.53	31.48	31.41333	0.160728
YZ	31.64	31.79	31.76	31.73	0.079373

All dimensions are in mm

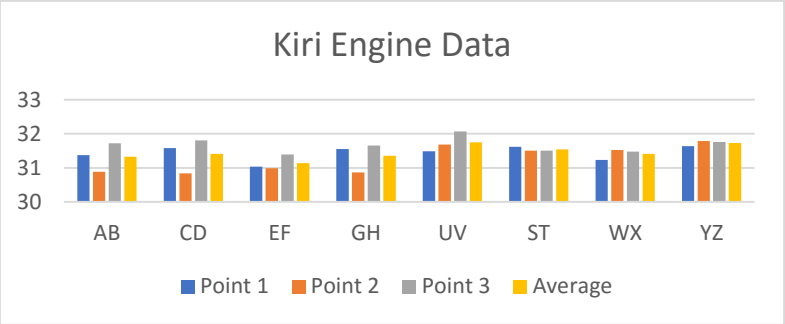

Figure 9: Bar Chart representation of Kiri Engine measurement Data

(All dimensions are in mm)

Table 7: The height of the cube at three different points is tabulated below

Height	Point 1	Point 2	Point 3	Average	STDEV
IJ	30.02	30.1	30.16	30.09333	0.070238
KL	30.15	30.13	29.91	30.06333	0.133167
MN	30.11	30.03	29.94	30.02667	0.085049
OP	30.04	30.04	30.15	30.07667	0.063509

All dimensions are in mm

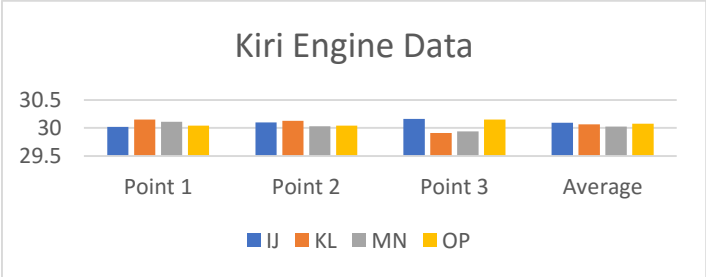

Figure 10: Bar Chart representation of Kiri Engine measurement Data
(All dimensions are in mm)

Also, measurement data of all the diagonals are tabulated below (All dimensions are in mm)

Diagonals	ab	cd	mn	op	qr	st	wx	uv	ef
Value	42.03	43.40	42.40	43.18	42.76	42.89	43.34	43.44	42.44

Diagonals	gh	ij	kl	Cf	ag	Ve	Wh	Kc	jb
Value	42.71	42.52	42.66	50.68	49.38	50.93	51.43	49.87	51.38

Diagonals	Xq	Vt	Um	Xp	Wi	ul	Nb	Ob	rq
Value	50.21	49.55	51.63	50.43	50.45	49.57	49.67	49.85	49.81

Diagonals	sd
Value	50.62

3.9 Kiri Engine Experiment 2

A total of 200 photos were taken around the cylinder in a circle. Then all the photos were imported into the Kiri Engine for the photogrammetry process. Once the 3D model was generated, it was clean up in the Meshmixer software. The 3D model was sliced in Ultimaker Cura 5.0.0 and it was scaled as X-axis to 40mm, Y-axis to 39.114, and Z-axis to 38.146. The Y-axis and Z-axis were scaled automatically by the software. It was then printed by FDM as described earlier.

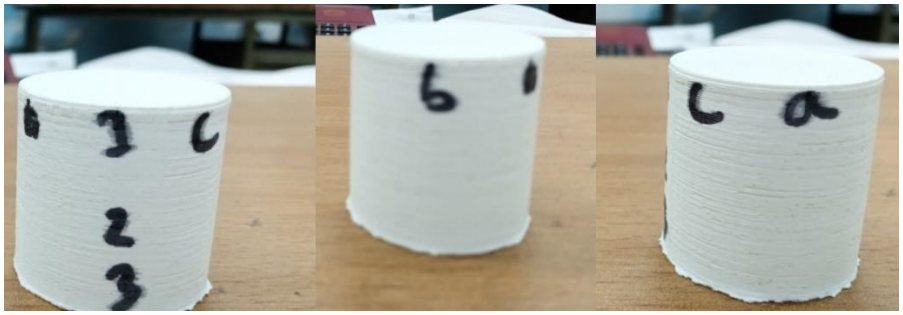

Figure 11: Photographic View of cylinder obtained by photogrammetry in Kiri Engine

The measurements of the heights at points a, b, and c are tabulated below (All dimensions are in mm)

Points	Height
a	39.46
b	39.74
c	39.48

The measurements of diameters at points 1, 2 and 3 are tabulated below (All dimensions are in mm)

Points	Diameter
1	39.46
2	38.98
3	38.86

3.10 Comparison between Autodesk Recap Pro and Kiri Engine App for the cube

Table 8: Autodesk Recap data (All dimensions are in mm)

Faces	Point 1	Point 2	Point 3	AVG	SDF
AB	29.08	28.58	28.87	28.84333	0.251064
CD	28.98	28.45	28.64	28.69	0.268514
EF	29.04	28.58	28.95	28.85667	0.24379
GH	29.01	28.45	28.84	28.76667	0.287112

Faces	Point 1	Point 2	Point 3	AVG	SDV
ST	28.98	28.93	28.97	28.96	0.026458
UV	28.93	28.8	29.03	28.92	0.115326
WX	28.94	28.82	28.97	28.91	0.079373
YZ	28.96	28.86	29.26	29.02667	0.208167

Table 9: Kiri Engine Data (All dimensions are in mm)

Faces	Point 1	Point 2	Point 3	Average	STDEV
AB	31.38	30.89	31.72	31.33	0.417253
CD	31.58	30.84	31.81	31.41	0.506853
EF	31.04	30.99	31.39	31.14	0.217945
GH	31.55	30.87	31.66	31.36	0.427902
UV	31.49	31.69	32.07	31.75	0.294618
ST	31.62	31.51	31.51	31.54667	0.063509
WX	31.23	31.53	31.48	31.41333	0.160728
YZ	31.64	31.79	31.76	31.73	0.079373

Table 10: Autodesk Recap Pro data (All dimensions are in mm)

Height	Point 1	Point 2	Point 3	AVG	SDV
IJ	27.11	27.32	27.44	27.29	0.167033
KL	27.55	27.41	27.38	27.44667	0.090738
MN	27.61	27.36	27.1	27.35667	0.255016
OP	27.42	27.35	27.47	27.41333	0.060277

Table 11: Kiri Engine data (All dimensions are in mm)

Height	Point 1	Point 2	Point 3	Average	STDEV
IJ	30.02	30.1	30.16	30.09333	0.070238
KL	30.15	30.13	29.91	30.06333	0.133167
MN	30.11	30.03	29.94	30.02667	0.085049
OP	30.04	30.04	30.15	30.07667	0.063509

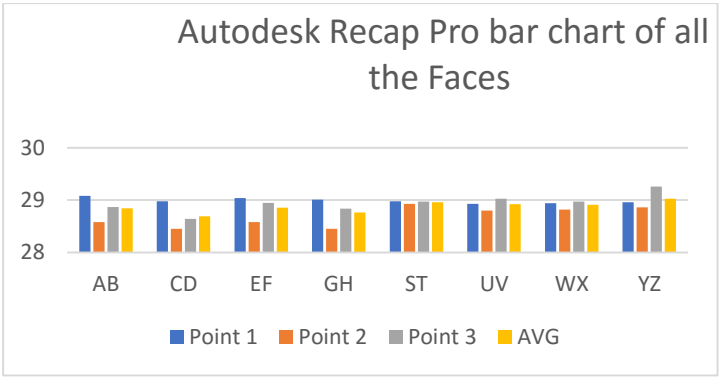

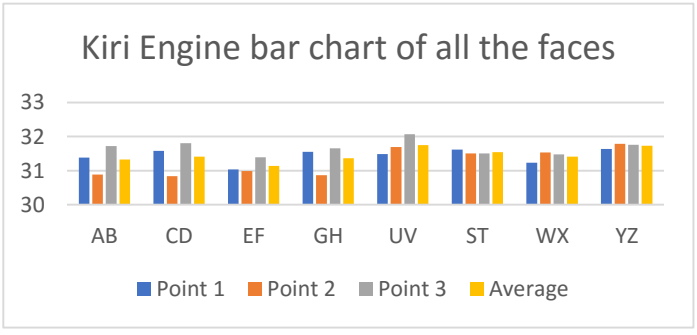

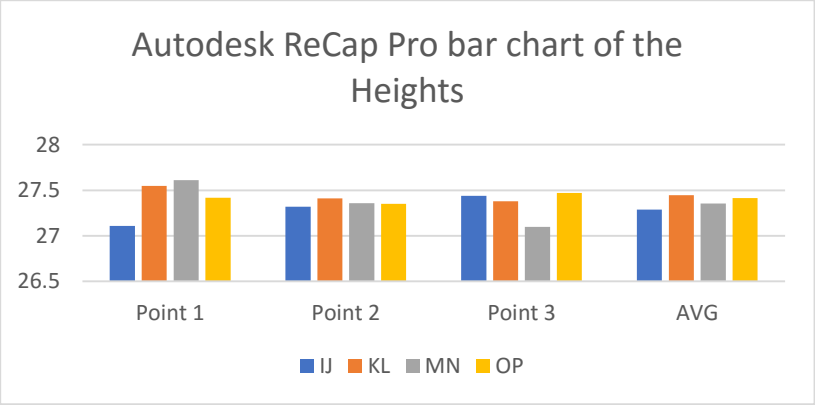

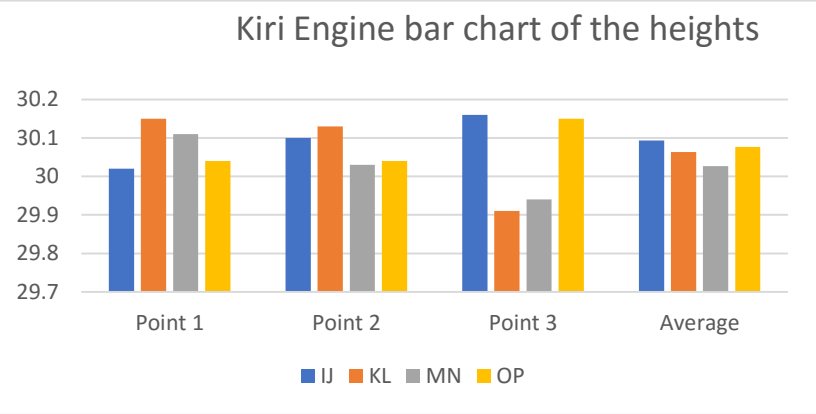

The STDEV comparison of the faces of the cube between Autodesk recap pro and Kiri Engine has been shown in table 12 below.

Table 12: STDEV of the faces of the cube (All dimensions are in mm)

Faces	STDEV of Autodesk	STDEV of Kiri Engine
AB	0.251064	0.417253
CD	0.268514	0.506853
EF	0.24379	0.217945
GH	0.287112	0.427902
ST	0.026458	0.294618
UV	0.115326	0.063509
WX	0.079373	0.160728
YZ	0.208167	0.079373

The STDEV comparison of the heights of the cube between Autodesk Recap and Kiri Engine has been shown in table 13 below.

Table 13: STDEV of the heights of the cube (All dimensions are in mm)

Heights	STDEV of Autodesk	STDEV of Kiri
IJ	0.167033	0.070238
KL	0.090738	0.133167
MN	0.255016	0.085049
OP	0.060277	0.063509

Figure 12, shown the STDEV comparison bar chart of all the faces of the cube between Autodesk Recap Pro and Kiri Engine App has been shown below.

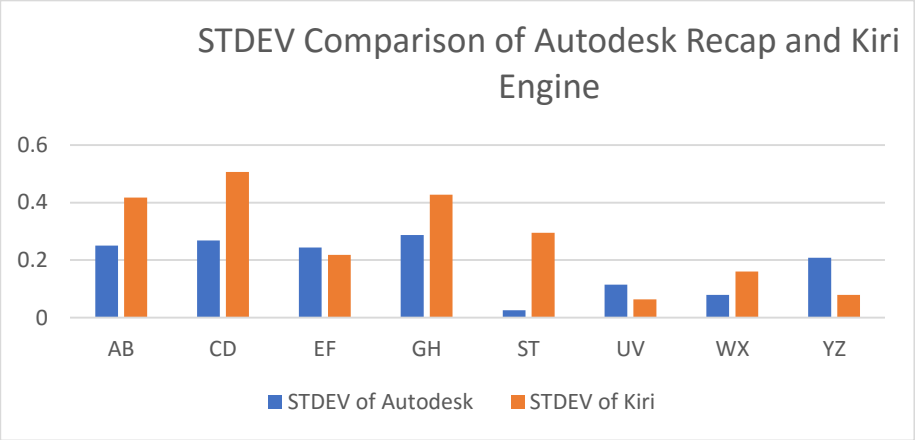

Figure 12: Standard deviation comparison between Autodesk Recap pro faces and Kiri Engine faces of the cube (All dimensions are in mm)

Figure 13, shown the STDEV comparison bar chart of the heights of the cube between Autodesk Recap Pro and Kiri Engine App has been shown below.

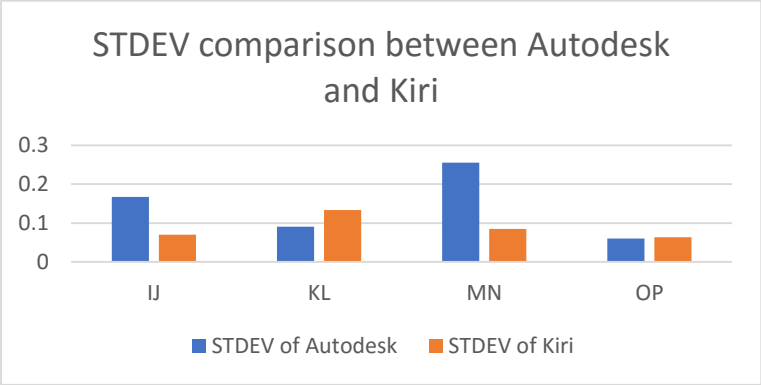

Figure 13: Standard deviation comparison between Autodesk Recap pro heights and Kiri Engine heights of the cube (All dimensions are in mm)

3.11 Comparison between Autodesk Recap Pro and Kiri Engine App for cylinder

Table 14: Comparison of Autodesk Recap diameter and Kiri Engine diameter (All dimensions are in mm)

	Autodesk Recap Diameter	Kiri Engine diameter
	41.43	39.46
	40.63	38.98
	40.4	38.86
STDEV	0.54064776	0.317490157

Table 15: Comparison of Autodesk Recap height and Kiri Engine height (All dimensions are in mm)

	Autodesk Recap Height	Kiri Engine height
	39.4	39.46
	39.13	39.74
	39.17	39.48
STDEV	0.14571662	0.156204994

Figure 14 shown the STDEV of Autodesk Recap pro diameter and STDEV of Kiri Engine diameter of the cylinder (All dimensions are in mm)

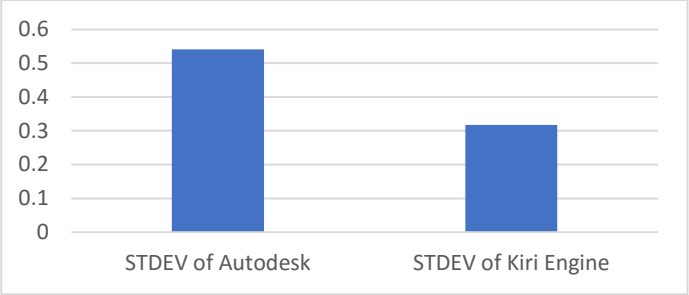

Figure 14: STDEV of the diameter of the cylinder between Autodesk Recap and Kiri Engine

Figure 15 shown the STDEV of Autodesk Recap pro height and STDEV of Kiri Engine height of the cylinder (All dimensions are in mm)

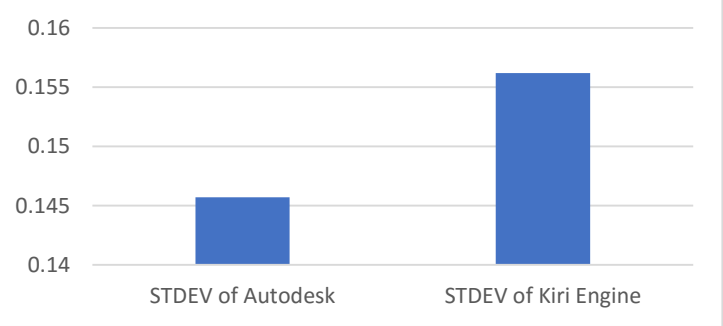

Figure 15: STDEV of the height of the cylinder between Autodesk Recap and Kiri Engine

3.11 Results and Discussion

In this experiment, it is observed that the values obtained in Autodesk ReCap Pro and the values obtained in Kiri Engine App are slightly different from each other. It is also observed that the accuracy of photogrammetry is directly proportional to the STDEV. The less STDEV means the 3D model is more accurate. By comparing STDEV from tables 12 and 13, it is concluded that Kiri Engine is more accurate for a cylindrical shape. By comparing tables 8,9,10 and 11, 12, it is concluded that Autodesk recap pro is more accurate for cubes.

Chapter 4

4. Distortion and Accuracy measurement

4.1 Distortion and Accuracy measurement of the cube

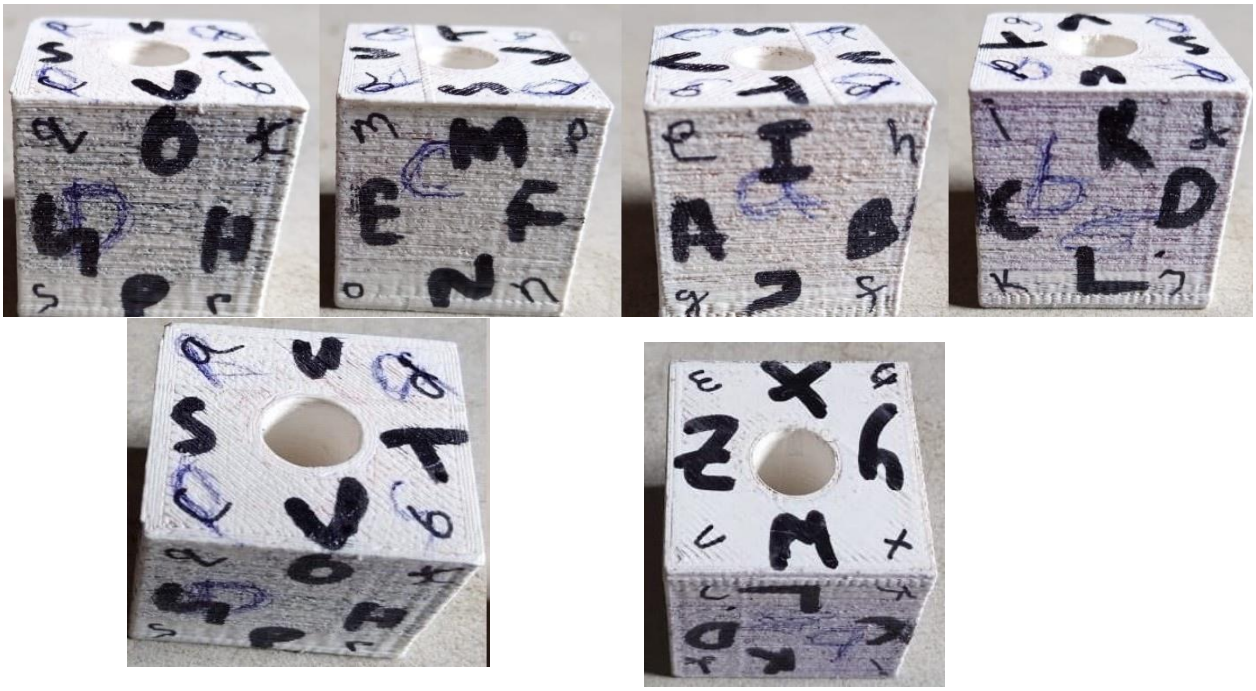

Figure 16: Photographic view of the actual cube

In table 16, the measurement value of all the faces of the actual cube is tabulated

Table 16: Measurement values of all the faces of the cube (All dimensions are in mm**)**

Faces	Point 1	Point 2	Point 3	Average	STDEV
AB	30.21	30.25	30.72	30.39333	0.283608
CD	30.13	30.2	30.52	30.28333	0.207926
EF	30.25	30.22	30.6	30.35667	0.211266
GH	30.22	30.16	30.53	30.30333	0.198578
UV	30.5	30.58	30.4	30.49333	0.090185
ST	30.44	30.56	30.33	30.44333	0.115036
WX	30.56	30.64	30.73	30.64333	0.085049
YZ	30.53	30.57	30.53	30.54333	0.023094

.

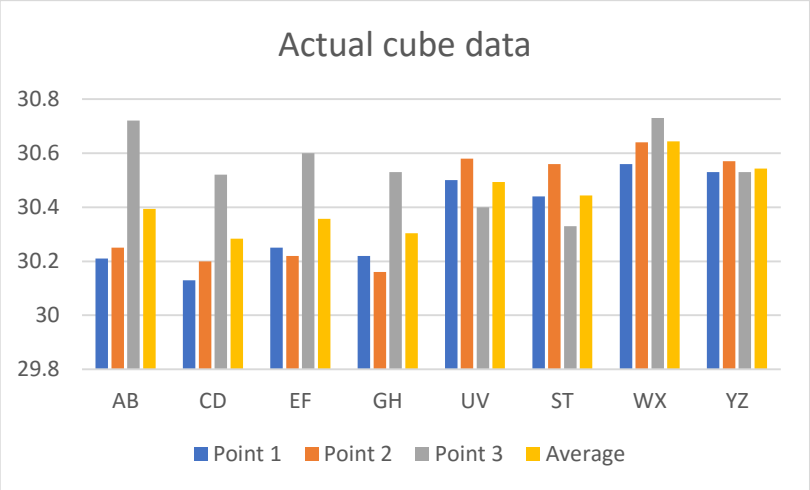

Figure 17: Bar Chart representation of the faces of the actual cube data (All dimensions are in mm)

Table 17: The heights of the actual cube at three different points are tabulated below

Heights	Point 1	Point 2	Point 3	Average	STDEV
IJ	30.07	30.09	30.11	30.09	0.02
KL	30.17	30.14	30.19	30.16667	0.025166
MN	30.15	30.05	30.06	30.08667	0.055076
OP	30.14	30.16	30.12	30.14	0.02

All dimensions are in mm

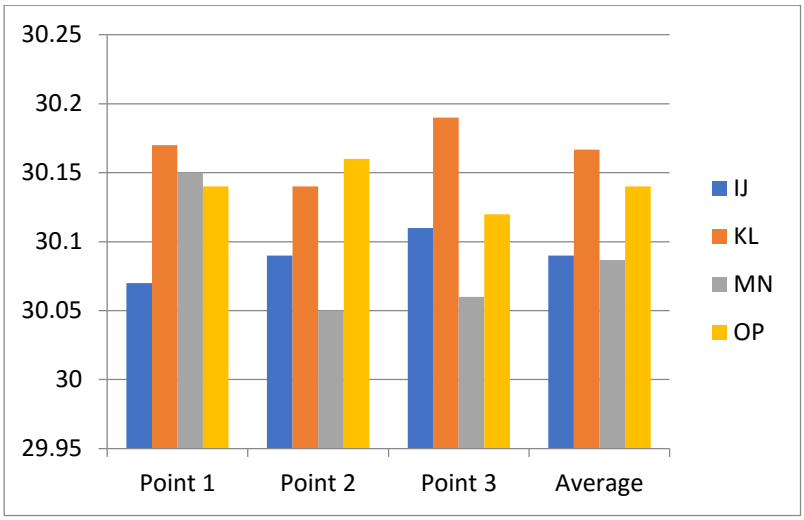

Figure 18: Bar chart representation of the heights of the actual cube (All dimensions are in mm)

The diagonal measurement of the actual is tabulated (All dimensions are in mm)

Diagonals	Mu	Px	Qx	Tv	Ev	Hw	Iw	Lu	nd
Value	49.43	50.13	48.77	48.42	48.51	49.55	51.07	49.58	49.93

Ob	Ja	Kc	Fc	Ga	Ar	sd
49.23	49.76	50.26	50.48	50.68	49.59	50.62

Figure 19, shown the STDEV comparison of the faces among Autodesk recap, Kiri Engine and the actual cube

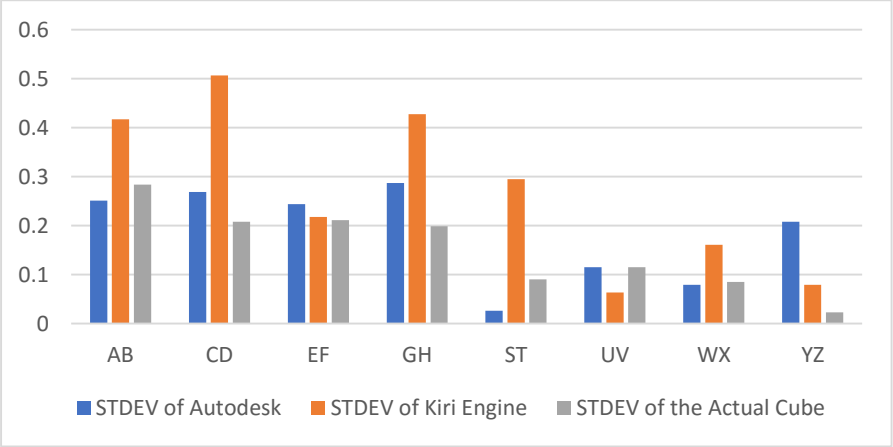

Figure 19: STDEV comparison of the faces (All dimensions are in mm)

Table 18, shows the STDEV comparison of the faces among Autodesk recap, Kiri Engine and the actual cube

Table 18: STDEV comparison table (All dimensions are in mm)

Faces	STDEV of Autodesk	STDEV of Kiri Engine	STDEV of the Actual Cube
AB	0.251064	0.417253	0.283608
CD	0.268514	0.506853	0.207926
EF	0.24379	0.217945	0.211266
GH	0.287112	0.427902	0.198578
ST	0.026458	0.294618	0.090185
UV	0.115326	0.063509	0.115036
WX	0.079373	0.160728	0.085049
YZ	0.208167	0.079373	0.023094

Figure 20, shown the STDEV comparison of the heights among Autodesk recap, Kiri Engine and the actual cube (All dimensions are in mm)

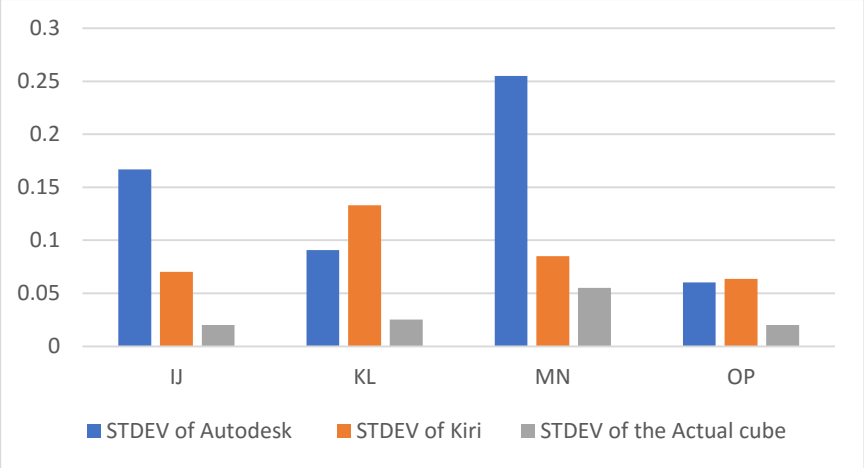

Figure 20: STDEV comparison of the heights

Table 19 shown the STDEV comparison of the heights among Autodesk recap, Kiri Engine and the actual cube

Table 19: STDEV comparison of the heights (All dimensions are in mm)

Heights	STDEV of Autodesk	STDEV of Kiri	STDEV of the Actual cube
IJ	0.167033	0.070238	0.02
KL	0.090738	0.133167	0.025166
MN	0.255016	0.085049	0.055076
OP	0.060277	0.063509	0.02

Tables 20 and 21 compared the error between the actual cube and the Autodesk Recap Pro 3D model.

Table 20: Error of all the faces of the cube (All dimensions are in mm)

Faces	Actual cube	Autodesk Recap	Error
AB	30.3933	28.84333	1.54997
CD	30.2833	28.69	1.5933
EF	30.3567	28.85667	1.50003
GH	30.3033	28.76667	1.53663
UV	30.4933	28.96	1.5333
ST	30.4433	28.92	1.5233
WX	30.6433	28.91	1.7333
YZ	30.5433	29.02667	1.51663

Table 21: Error of the heights of the cube (All dimensions are in mm)

Height	Actual cube	Autodesk Recap	Error
IJ	30.09	27.29	2.8
KL	30.1667	27.44667	2.717
MN	30.08667	27.35667	2.703
OP	30.14	27.41333	2.7267

Tables 22 and table 23 compared the error between the actual 3D model and the Kiri Engine 3D model

Table 22: Error of all the faces of the cube (All dimensions are in mm)

Faces	Actual cube	Kiri Engine	Error
AB	30.3933	31.33	0.9367
CD	30.2833	31.41	1.1267
EF	30.3567	31.14	0.7833
GH	30.3033	31.36	1.0567
UV	30.4933	31.75	1.2567
ST	30.4433	31.54667	1.10337
WX	30.6433	31.41333	0.77003
YZ	30.5433	31.73	1.1867

Table 23: Error of the heights of the cube (All dimensions are in mm)

Height	Actual cube	Kiri Engine	Error
IJ	30.09333	30.09	0.00333
KL	30.06333	30.16667	0.10334
MN	30.02667	30.08667	0.06
OP	30.07667	30.14	0.06333

4.2 Distortion and Accuracy measurement of the cylinder

Figure 21: Photographic view of the actual cylinder

Table 24: Diameters of the actual 3D model at points 1, 2, and 3 are tabulated below

Points	Diameter(mm)
1	40.09
2	40.01
3	40.05

Table 25: Heights of the actual 3D model at points a, b, and c are tabulated below

Points	Height(mm)
a	40.09
b	40.11
c	40.10

Tables 26 and 27 represent the error of the cylinder between the actual 3D model and the Kiri Engine 3D model

Table 26: Error of the diameter of the cylinder (All dimensions are in mm)

Diameter	Kiri Engine	Actual cylinder	Error
1	39.46	40.09	0.63
2	38.98	40.01	1.03
3	38.86	40.05	1.19

Table 27: Error of the heights of the cylinder (All dimensions are in mm)

Heights	Kiri Engine	Actual cylinder	Error
1	39.46	40.09	0.63
2	39.74	40.11	0.37
3	39.17	40.1	0.93

Tables 28 and 29 represent the error of the cylinder between the actual 3D model and the Autodesk Recap Pro 3D model

Table 28: Error of the diameter of the cylinder (All dimensions are in mm)

Diameter	Autodesk Recap	Actual cylinder	Error
1	41.43	40.09	1.34
2	40.63	40.01	0.62
3	40.4	40.05	0.35

\

Table 29: Error of the heights of the cylinder (All dimensions are in mm)

Heights	Autodesk Recap	Actual cylinder	Error
1	39.4	40.09	0.69
2	39.13	40.11	0.98
3	39.17	40.1	.93

4.3 Distortion Measurement

Table 30 shown the distortion of the cylinders

Table 30: Distortion of the cylinders (All dimensions are in mm)

Cylinder	Maximum Diameter	Minimum Diameter	Distortion
Actual Cylinder	40.09	40.01	0.08
Autodesk Cylinder	41.43	40.4	1.03
Kiri Engine Cylinder	39.46	38.86	0.6

Table 31 shown the diagonal distortion of the actual cube and Kiri Engine
Table 31: Distortion of the actual cube and Kiri Engine cube (All dimensions are in mm)

Diagonals	Actual cube	Kiri Engine	Distortion
AB	41.99	43.2	1.21
CD	41.6	43.25	1.65
EF	42.38	43.22	0.84
GH	42.27	43.68	1.41
IJ	42.11	42.59	0.48
KL	41.1	41.59	0.49
MN	42.29	42.33	0.04
OP	42.11	42.33	0.22
QR	42.67	43.15	0.48
ST	42.31	43.59	1.28
UV	41.7	43.08	1.38
WX	41.78	42.91	1.13

Table 32 shown the diagonal distortion of the actual cube and Autodesk Recap cube
Table 32: Distortion of the actual cube and Autodesk recap cube (All dimensions are in mm)

Diagonals	Actual cube	Autodesk Recap cube	Distortion
AB	41.99	42.15	0.16
CD	41.6	42.17	0.57
EF	42.38	42.22	0.16
GH	42.27	42.7	0.43
IJ	42.11	42.49	0.38
KL	41.1	41.3	0.2
MN	42.29	41.33	0.96
OP	42.11	42.56	0.45
QR	42.67	41.15	1.52
ST	42.31	42.59	0.28
UV	41.7	41.08	0.62
WX	41.78	41.68	0.1

4.4 Results and Discussion

By close analysis of all the errors, it is concluded that the accuracy of the photogrammetry varies from software to software.
By analysis of the diagonal distortion of the Autodesk recap cube and Kiri Engine cube with the actual cube, it has been found that Autodesk is more accurate than Kiri Engine for a cube.
Also, in the case of a cylindrical object, the Kiri engine gives a more accurate 3D model than Autodesk recap pro.

Chapter 5

5. Human face modelling

There is a need for accurate anthropometric data of the human head and face for both research and product design. In the past conventional measurement, techniques were used to acquire anthropometric measurements for designing products using scales, callipers, and tapes which were less accurate and reliable, but with the advent of the 3D scanner, it has become very convenient for researchers to acquire accurate 3D anthropometric head and face measurement. In the last three decades, there has been a constant effort in optimizing 3D scanners for improving their accuracy and making them more user-friendly. In this experiment, photogrammetry is used for scanning human faces and the performance of photogrammetry for human face modelling is analysed.[44]

5.1 Equipment Needed for this experiment

1. Mobile Camera
2. Computer
3. Operating System
4. Photogrammetry Software
5. Ultimaker Cura 5.0.0
6. FDM (Fused Deposition Modeling)
7. PLA
8. Object

5.2 Equipment details

1. **Mobile Camera**: 16M QUAD camera of Infinix hot 10 Mobile
2. **Computer**
    - Device name DESKTOP-71D3QVG
    - Processor Intel® Core™ i5-7500
    - CPU 3.40 GHz 3.41 GHz
    - RAM 8GB
    - System type 64-bit operating system, x64-based processor
3. **Operating system**: Windows 10 pro
4. **Photogrammetry Software:** Autodesk ReCap Pro 2023
5. **Ultimaker Cura 5.0.0**

    Ultimaker Cura is the world's most popular 3D printing software, integrate with CAD software for an easier workflow, or dive into custom settings for in-depth control.

6. **Object**: In this experiment, a human face is used as an object for 3D printing.

5.3 Equipment Setup: Autodesk recap pro and Ultimaker Cura were installed onto the computer for the experimental procedures. FDM is also set up for 3D printing.

5.4 Experiment procedure

A series of overlapping photos were taken in a circle around the human face using Infinix hot 10 smartphone's 16MP quad-camera. Shooting around an object is the most effective as reference points in the background help the software properly orient the photos in space. A total of 220 photos were taken for this experiment. Then all the photos were imported into Autodesk Recap pro software for further processing.

Since it is cloud-based software, all the steps of photogrammetry proceeded automatically. After processing is done, a 3D mesh file of the human face is generated as shown in the image below.

Figure 22: Photographic view of 3D mesh generated in the Autodesk Recap pro

Then, all the unwanted objects were edited out by the "edit" tool of the software.

After cleaning up those unwanted objects, a 3D model was ready.

Figure 23: Photographic View of the 3D model generated in the software

Then the 3D model is converted to the STL format and imported into the "Ultimaker Cura" for slicing and scaling.

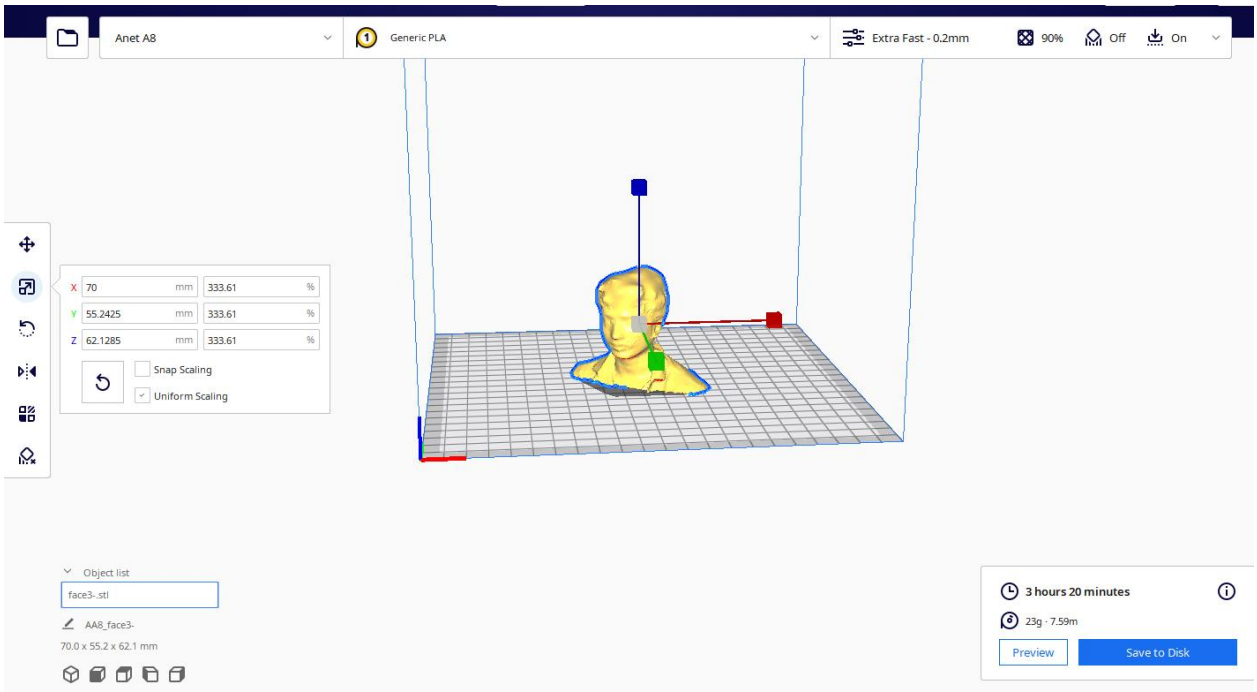

Figure 24: Photographic view of slicing in Ultimaker Cura

Dimensions of the model after scaling are as follows:

X-axis -70mm, Y-axis-55.2425mm, Z -axis 62.1285mm.

And the total of 200 minutes is required for the FDM to print the model at a speed of 50mm/s.

FDM starts 3D printing when the printing temperature and the build plate temperature reach 210°C and 60°C respectively

5.5 Results and Discussion

Figure 25 depicted the result of the scanned output for a human face using photogrammetry. Based on the result, it is concluded that accurate face modelling is possible by photogrammetry. But various factors need to be considered during face modelling such as scanner accuracy, time and process of data acquisition and processing, the advantages and the limitations of the scanner and possible applications of the scanners and user-friendliness.

Figure 25: Photographic view of the 3D print model of the object and the original object

Chapter 6

6. Summary and General conclusion

In the present study different 3D scanning technologies for creating 3D models of real-world objects were studied and it was noted that each 3D scanning technology comes with its limitations, advantages, and costs. It is observed that photogrammetry is one of the cheapest 3D scanning options available in the market that requires only a digital camera or smartphone and a software package. Different photogrammetric software packages available in the market have been explored. Among them, one high-end premium and comparatively costly software package Autodesk recap pro and another relatively cheaper software package Kiri Engine were considered in this study.

To compare the performance of this software, 3D scanning of one existing cube and cylinder were carried out. After 3D scanning, the physical models were created using a 3D printer and then those models were compared with that of the original model for measuring the comparative performance of these two photogrammetry software packages. Based on the experimental results it was observed that in terms of dimensional consistency, and surface quality, both the software are giving very good results. In some cases, Autodesk recap pro is giving better results and in some cases, Kiri engine is also giving better results. Besides dimensional consistency, the amount of distortion produced by photogrammetry software has been investigated. It was observed that in some cases (cube) Autodesk recap pro is giving marginally better results and in some cases, Kiri Engine is giving marginally better results. However, both the software exhibited fairly accurate results. Finally, in a case study, human face modelling was carried out using these photogrammetry and 3D printing technologies and obtained a very encouraging result. Thus, both the software are quite efficient and accurate but from the price point of view, Kiri Engine ($USD57 annually) is way cheaper than Autodesk's $USD215 recap pro package.

Thus, it is finally concluded that Kiri Engine is a potential cheap 3d scanning solution and it radically lowers the barrier to entry for those wanting to create detailed digital 3D models and recreate them using a 3D printer.

References

1. https://www.aniwaa.com/guide/3d-scanners/3d-scanning-technologies-and-the-3d-scanning-process/
2. https://www.ems-usa.com/3d-knowledge-center/3d-scanning-knowledge-center/types-of-3d-scanners-and-3d-scanning-technologies/
3. https://www.linkedin.com/pulse/types-3d-scanning-technologies-scanners-karan-kamani
4. https://www.3dnatives.com/en/top-10-low-cost-3d-scanners280320174/#!
5. J. Horswell, Encyclopedia of Forensic Sciences, Recordings, 2013, Pages 368-371, https://doi.org/10.1016/B978-0-12-382165-2.00207-5
6. James S. AberIrene, Marzolff Johannes, B. Ries, Small-Format Aerial Photography, Principles, Techniques, and Geoscience Applications, Photogrammetry, 2010, Pages 23-39, https://doi.org/10.1016/B978-0-444-53260-2.10003-1
7. The centre for photogrammetric Training, History of Photogrammetry, Early developments, pages 2-36, https://ibis.geog.ubc.ca/courses/geob373/lectures/Handouts/History_of_Photogrammetry
8. Pete Bettinger, Kevin Boston Jacek P. Siry, Donald L. Grebner, Forest Management and Planning (Second Edition), Geographic Information and Land Classification in Support of Forest Planning, 2017, Pages 65-85, https://doi.org/10.1016/B978-0-12-809476-1.00003-5
9. https://formlabs.com/asia/blog/photogrammetry-guide-and-software-comparison/
10. https://www.vedantu.com/geography/photogrammetry
11. https://www.photomodeler.com/kb/factors_affecting_accuracy_in_photogramm/
12. S.N. Lane, The Measurement of River Channel Morphology Using Digital Photogrammetry, The Photogrammetric Record, 2000, Volume 16, Issue 96, Pages 937-961, https://doi.org/10.1111/0031-868X.00159
13. Ayse Gulcin Kucukkaya, Journal of Quantitative Spectroscopy and Radiative Transfer, Photogrammetry and remote sensing in archaeology, Volume 88, Issues 1–3, 2004, Pages 83-88, https://doi.org/10.1016/j.jqsrt.2003.12.030
14. P.Arias, J.Herráez, H.Lorenzo, C.Ordóñeza, Computers & Structures, Control of structural problems in cultural heritage monuments using close-range photogrammetry and computer methods, Volume 83, Issues 21–22, 2005, Pages 1754-1766 https://doi.org/10.1016/j.compstruc.2005.02.018
15. De-hai Zhang, Liang Jin, Cheng Guo, Jian-Wei Liu, Xiao-Qiang Zhang, Zhi-Xin Chen
    The exploitation of photogrammetry measurement system, Optical Engineering 49(3),2010, https://doi.org/10.1117/1.336405

16. Naci Yastikli, Journal of Cultural Heritage, Documentation of cultural heritage using digital photogrammetry and laser scanning, Volume 8, Issue 4, 2007, Pages 423-427
https://doi.org/10.1016/j.culher.2007.06.003
17. Ruining Jiang, David V.Jáuregui, Kenneth R.White, Measurement, Close-range photogrammetry applications in bridge measurement: Literature review, Volume 41, Issue 8, 2008, Pages 823-834, https://doi.org/10.1016/j.measurement.2007.12.005
18. Clive S. Fraser, Simon Cronk, ISPRS Journal of Photogrammetry and Remote Sensing, A hybrid measurement approach for close-range photogrammetry, Volume 64, Issue 3, 2009, Pages 328-333, https://doi.org/10.1016/j.isprsjprs.2008.09.009
19. Muammer Ozbeka, Daniel J.Rixen, Oliver Erneb, Gunter Sanowb
Energy, Feasibility of monitoring large wind turbines using photogrammetry, Volume 35, Issue 12, 2010, Pages 4802-481, https://doi.org/10.1016/j.energy.2010.09.008
20. Thomas Luhmann, ISPRS Journal of Photogrammetry and Remote Sensing, Close range photogrammetry for industrial applications, Volume 65, Issue 6, 2010, Pages 558-569
https://doi.org/10.1016/j.isprsjprs.2010.06.003
21. M.J.Westoby, J.Brasington, N.F.Glasser, M.J.Hambrey, J.M.Reynolds
Geomorphology, Structure-from-Motion photogrammetry: A low-cost, effective tool for geoscience applications, Volume 179, 15 December 2012, Pages 300-314
https://doi.org/10.1016/j.geomorph.2012.08.021
22. Armin Gruen, Development and Status of Image Matching in Photogrammetry, The Photogrammetric Record, Volume 27, Issue 137, 2012, Pages 36-57
https://doi.org/10.1111/j.1477-9730.2011.00671.x
23. M.Lato, J.Kemeny, R.M.Harrap, G.Bevand, Computers & Geosciences, Rock bench: Establishing a common repository and standards for assessing rock mass characteristics using LiDAR and photogrammetry, Volume 50, 2013, Pages 106-114
https://doi.org/10.1016/j.cageo.2012.06.014
24. M.Uysal, A.S.Toprak, N.Polata, Measurement, DEM generation with UAV Photogrammetry and accuracy analysis in Sahitler hill, Volume 73, 2015, Pages 539-543
https://doi.org/10.1016/j.measurement.2015.06.010
25. J.A. Gonçalves, R. Henriques, SPRS Journal of Photogrammetry and Remote Sensing, UAV photogrammetry for topographic monitoring of the coastal area, Volume 104, 2015, Pages 101-111, https://doi.org/10.1016/j.isprsjprs.2015.02.009
26. Birutė Ruzgienė, Tautvydas Berteška, Silvija Gečyte, Edita Jakubauskienė, Vladislovas Česlovas Aksamitauskas, Measurement, The surface modelling based on UAV Photogrammetry and qualitative estimation, Volume 73, 2015, Pages 619-627, https://doi.org/10.1016/j.measurement.2015.04.018

27. Satoshi Nishiyama, Nao Minakata, Teruyuki Kikuchi, Takao Yano, Advanced Engineering Informatics, Improved digital photogrammetry technique for crack monitoring, Volume 29, Issue 4, 2015, Pages 851-858 https://doi.org/10.1016/j.aei.2015.05.005
28. Thomas Luhmann, Clive Fraser, Hans-Gerd Maas, ISPRS Journal of Photogrammetry and Remote Sensing, Sensor modelling and camera calibration for close-range photogrammetry, Volume 115, 2016, Pages 37-46 https://doi.org/10.1016/j.isprsjprs.2015.10.006
29. Janowski Artur, Nagrodzka Godycka, and Ziolkowski Patryk, Computers and Concrete, Remote sensing and photogrammetry techniques in diagnostics of concrete structures, Volume 18, Issue 3, 2016, Pages 405-420, https://doi.org/10.12989/cac.2016.18.3.405
30. B.Kršák, P.Blišťan, A. Pauliková, P.Puškárová, Measurement, Use of low-cost UAV photogrammetry to analyze the accuracy of a digital elevation model in a case study, Volume 91, 2016, Pages 276-287, https://doi.org/10.1016/j.measurement.2016.05.028
31. Javad Baqersad, Peyman Poozesh, Christopher Niezrecki, Peter Avitabile, Mechanical Systems and Signal Processing, Photogrammetry and optical methods in structural dynamics – A Review, Volume 86, Part B, 2017, Pages 17-34 https://doi.org/10.1016/j.ymssp.2016.02.011
32. Jacob A. Morgan, Daniel J. Brogan, and Peter A. Nelson, Geomorphology, Application of Structure-from-Motion photogrammetry in laboratory flumes, Volume 276, 2017, Pages 125-143, https://doi.org/10.1016/j.geomorph.2016.10.021
33. Hany Omar, Lamine Mahdjoubi, and Gamal Kheder, Computers in Industry, Towards an automated photogrammetry-based approach for monitoring and controlling construction site activities, Volume 98, Pages 172-182, https://doi.org/10.1016/j.compind.2018.03.012
34. I. Colomina, P.Molina, ISPRS Journal of Photogrammetry and Remote Sensing, Unmanned aerial systems for photogrammetry and remote sensing: A review, Volume 92, Pages 79-97, https://doi.org/10.1016/j.isprsjprs.2014.02.013
35. Jakob Iglhaut, Jakob Iglhaut, James O'Connor Remote Sensing, Structure from Motion Photogrammetry in Forestry: a Review Volume 5, Issue 3, 2019, Pages 155-168, https://doi.org /10.1007/s40725-019-00094-3
36. Hashem Mohammad Khris, Photogrammetry versus 3D scanner: producing 3D models of museums' artefacts, Volume 40 NO. 4, Pages 153-157 https://doi.org/10.1108/CC-06-2020-0021
37. https://www.nikonmetrology.com/en-us/3d-metrology/automated-3d-scanning-l100
38. https://knowledge.autodesk.com/support/recap/troubleshooting/caas/sfdcarticles/sfdcarticles/System-requirements-for-Autodesk-ReCap-Pro-and-ReCap-Photo.html%20
39. https://www.autodesk.in/products/recap/overview?mktvar002=afc_in_deeplink&AID=13084956&PID=8206971&SID=jkp_EAIaIQobChMIoPOZ9Zzh-AIV8JJmAh2YYwvVEAAYASAAEgLKzPD_BwE&cjevent=296ce00efc3411ec8393

71700a18050f&affname=8206971_13084956&cjdata=MXxOfDB8WXww&term=1-YEAR&tab=subscription&plc=RECAP
40. https://www.kiriengine.com/
41. https://alicevision.org/#meshroom
42. https://www.sculpteo.com/en/3d-learning-hub/3d-printing-software/photogrammetry-software/
43. https://www.iitk.ac.in/dordold/index.php?option=com_content&view=category&layout=blog&id=200&Itemid=219#:~:text=FDM%20works%20on%20an%20%22additive,the%20flow%20on%20and%20off
44. Parth B. Shah & Yan Luximon, Digital Human Modeling. Applications in Health, Safety, Ergonomics, and Risk Management: Ergonomics and Design, Review on 3D Scanners for Head and Face Modeling, volume 10286, 2017, pages 47-56